SAPIENZA
UNIVERSITÀ DI ROMA

PhD Program in Behavioral Neuroscience

PhD School in Neuroscience

Psychobiology and Psychopharmachology

Cycle XXX

Targeting NGF system to fight neuropathic pain: behavioral and immunohistochemical evidence in mice

PhD STUDENT

Elena Fiori

TUTOR

Prof. Andrea Mele

SUPERVISOR

Dott.ssa Flaminia Pavone

Academic year 2016/2017

INDEX

ABSTRACT

Background and Aims: it has been demonstrated that the anti-NGF αD11 and the anti-TrkA MNAC13 counteract neuropathic pain in mice. The aim of this study was to evaluate the duration of the action of the two antibodies and the structural and morphological alterations induced in central and peripheral nervous system.

Methods: Chronic Constriction Injury (CCI) of the sciatic nerve was performed in C57BL/6J mice. Mice were administered with αD11 or MNAC13 (70 or 100 μg/mouse/day) from day 3 until day 10 post-CCI. Analgesic effects were tested through Dynamic Plantar Aesthesiometer from day 3 to day 90. Spinal cords and sciatic nerves were collected at D3, D11, D24 and D90 for immunohistochemistry.

Results: αD11 and MNAC13 induce significant dose- and time-dependent analgesic effects: the antiallodynic effect was still present at D90 following the highest doses of both antibodies. Immunohistochemical analysis show significant differences in inflammatory and myelination markers between treated and control animals, treated animals showing reduced glial and mast cells activation and a better nerve regeneration.

Conclusions: Data obtained prove that: i) the analgesic effect of the antibodies αD11 and MNAC13 are extremely long-lasting, being observable more than two months after the end of the treatment and ii) the antiNGF and antiTrkA antibodies reduce inflammation and facilitate the regenerative processes. Therefore, our results strongly support the importance of considering the NGF system in the development of novel therapies to modulate and control neuropathy.

INTRODUCTION

Among the diverse painful conditions, neuropathic pain is particularly challenging to manage because of the heterogeneity of its aetiology, symptoms and underlying mechanisms (Beniczky et al. 2005).

Several conditions have in common neuropathic pain as a core symptom, which include diabetic neuropathy, post-herpetic neuralgia, trigeminal neuralgia, radicular pain, post-surgical chronic neuropathic pain, and neuropathic cancer pain.

The manifestations can be diverse and include allodynia (pain caused by a stimulus that does not normally provoke pain), hyperalgesia (an increased response to a painful stimulus), anesthesia dolorosa (pain felt in an anesthetic [numb] area or region), and sensory gain or loss (IASP 2011). Patients often describe the pain symptoms in terms of shooting, stabbing, like an electric shock, burning, tingling, tight, numb, prickling, itching and a sensation of pins and needles.

The commonly used pharmacological treatments include antidepressants (tricyclic antidepressants [TCAs], selective serotonin reuptake inhibitors [SSRIs] and serotonin–norepinephrine reuptake inhibitors [SNRIs]), antiepileptic (anticonvulsant) drugs, topical treatments and opioid analgesics. In addition to their potential benefits, all of these drug classes are associated with various adverse effects.

The need of novel treatments is strongly emerging, making it important to further investigate biological substrates of pain to point out new pathways and molecules to focus on.

Besides its involvement in nerve growth, survival and regeneration Nerve Growth Factor (NGF) plays an important role in pain perception and maintenance.

Several studies on the blockade of its pathways have been performed to develop antihyperalgesic compounds.

We previously demonstrated that the administration of antibodies against NGF, αD11, and its receptor TrkA, MNAC13, counteracts inflammatory and neuropathic pain in mice. The aim of the present study, part of the project "Paincage: The NGF System and its interplay with endocannabinoid signalling, from peripheral sensory terminals to the brain: new targets for the development of next generation drugs for neuropathic pain" funded by the Seventh Framewok Programme of the European Commisson, will be to evaluate in a mouse model of neuropathic pain: i) how long the antihyperalgesic effects are maintained after the treatment and ii) if structural and morphological changes in central and peripheral nervous system occur.

Chapter I: Pain

The International Association for the Study of Pain (IASP) defines pain as "an unpleasant sensory and emotional experience associated with actual or potential tissue damage, or described in terms of such damage". Each individual learns through experiences related to injury in early life. Accordingly, pain is that experience we associate with actual or potential tissue damage. Pain has therefore a strong emotional component and the intensity of pain a subject perceives is conditioned by the milieu; the same noxious stimulus might in fact produce different response in different subjects.

There are different way of classifying pain, according to the involved components and the temporal persistence. It is possible to classify pain as inflammatory, visceral, neuropathic or oncologic.

These conditions may occur frequently and be maintained for prolonged periods and lead to the development of a pathological state, known as sensitization, that can alter neural substrate and therefore behavioral outcome, and is defined by IASP as "increased responsiveness of nociceptive neurons to their normal input, and/or recruitment of a response to normally subthreshold inputs". Sensitization can be central, referred to Central Nervous System (CNS), or peripheral, referred to Peripheral Nervous System (PNS); in both cases clinically sensitization may only be inferred from non-physiological painful states such as hyperalgesia or allodynia.

With the term hyperalgesia is defined a state in which higher pain is perceived from a stimulus that normally causes pain, while allodynia identifies pain provoked by stimuli that usually are harmless.

Focusing on the pain duration, we can identify acute pain, which is provoked by a specific disease or injury, serves a useful biologic purpose and is self-limited, and chronic pain, that may be considered a disease state; in this case pain outlasts the normal time of healing, if associated with a disease or injury. Chronic pain serves no biologic purpose, and has no recognizable end-point (Grichnik KP & Ferrante FM, 1991).

1.1 Neuropathic pain

Among different forms of chronic pain, neuropathic pain is a form of neurogenic pain arising as a direct consequence of a lesion or disease affecting the somatosensory system (Treede RD et al., 2008). This type of pain is different from the others, since the pain perception system is damaged itself and results to be activated with no “real” reason, spontaneously generating painful sensations, and it is often impossible to reverse this state. Approximately 100 million people in USA suffer from chronic neuropathic pain with serious impairment of the quality of life and extremely high cost in the public health, estimated around 600billion US dollars (Gaskin DJ & Richard P, 2012).

After nerve or tissue lesion, several neurophysiological processes occur giving rise to hyperexcitablity of neurons, leading to persistent pain perception.

Primary sensory neurons are responsible for detection and transduction of painful stimuli. Persistent nociceptive inputs after lesions result in increased response of the system to stimuli or in activity-dependent plasticity. These plastic changes, as already mentioned, can occur in

peripheral and central nervous system and are often closely related since the neuropathic mechanism can expand during the progression; after a peripheral damage pain signal originates from lesioned axons, but then the sensitization goes up to Dorsal Root Ganglia (DRG) to dorsal horns of spinal cord, up to cortical level.

1.1.1 Peripheral level

Peripheral neuropathic pain is frequently observed in patients with cancer, AIDS, long-standing diabetes, lumbar disc syndrome, herpes infection, traumatic spinal cord injury (SCI), multiple sclerosis and stroke. Moreover, peripheral neuropathy is often associated with several surgical practices.

The essential events of peripheral sensitization are hyperexcitability and sensitization of primary sensory neurons. After damage fiber degeneration occurs, together with alterations of channels expression and composition, resulting in ectopic firing and irregular signal transmission. Of primary importance in this process are voltage-gated Na^+ (Na_v) channels, in fact modifications of function, leading to faster activation and increased current density, increased expression and trafficking of several isoforms, account for hyperexcitation of peripheral nerves fibers, such as tiny myelinated Aδ fibers and unmyelinated C fibers (Liu M & Wood JN, 2011).

These processes, taking rise from a lesion in the axons of nerves, lead to several reactions aimed at axonal regeneration.

In basal condition the axons' cytoskeletal composition is regulated by specific glial cells, Schwann cells. They also provide support for axons

and form compact myelin sheaths around them to accelerate electrical propagation.

Axonal damage causes a process known as Wallerian degeneration (Waller A, 1850). This process occurs fast after the insult and is characterized by dismantling and clearance of injured axons and their myelin sheaths, glial cells proliferation, change in Blood-Nerve-Barrier (BNB) permeability as well as infiltration and activation of macrophages.

Schwann cells can "sense" axonal injury and within few minutes undergo a series of reactive changes in response. Schwann cells activation lead to myelin ovoid formation, process characterized by disassembly and digestion of the damaged myelin, to macrophage recruitment and nerve tissue remodeling (Cattin AL & Lloyd AC, 2016).

Responses aimed at promoting lisosomal/autophagic digestion of axons also take place, together with the activation of resident macrophage through the release of chemoattractants, such as tumor necrosis factor α (TNF-α), citokines, prostaglandins, Nerve Growth Factor (NGF) and glial cell-derived neurotrophic factor (GDNF).

Following the activation of resident macrophages further monocytes from peripheral blood stream are recruited. The damaged axons also release Calcitonin Gene Related Peptide (CGRP), substance P, bradikinin and nitric oxide, causing swelling and hyperaemia. These processes further support immune cells invasion, such as macrophages, T lymphocytes and Mast cells.

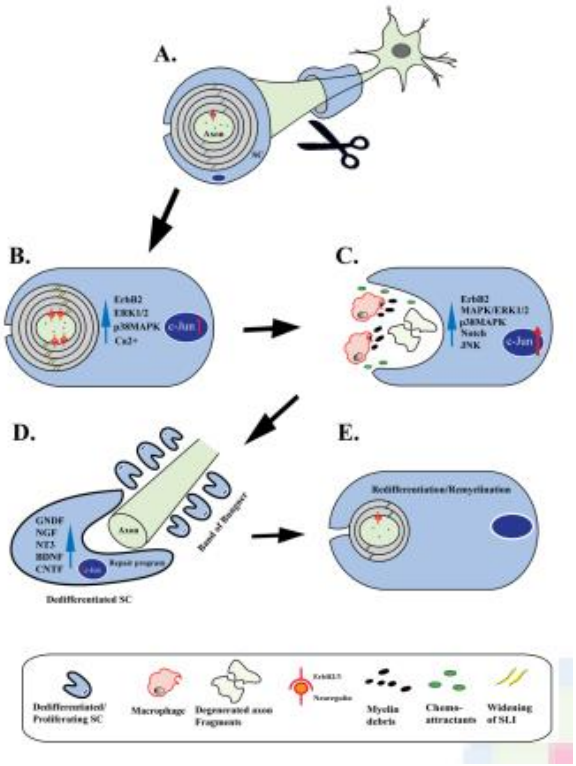

Figure 1. Schwann cell responses following lesion (Wong et al., 2017)

(A) Axon is encapsulated by a compact myelin sheath (B) Upon injury the first reactions in the Schwann cells: activation of the ErbB2 receptor tyrosine kinase, activation of p38- and Erk1/2 mitogen-activated protein kinase (MAPK) signaling, and rapid increase of cytoplasmic calcium levels. Increased expression of c-Jun is also observed few hours after nerve injury. These changes are accompanied by hypertrophy. (C) Axons abruptly disintegrate leaving fragments behind. In parallel, during Wallerian degeneration (WD) there is formation of myelin. Schwann cells release cytokines and chemokines that attract macrophages. (D) Axonal regeneration following WD is underway with neurotrophic factors. (E) Schwann cells conclude their repair program and redifferentiate to promote completion of nerve repair.

While the fragmentation and disintegration of axons begins, Schwann cells start to re-organize and activate a dedifferentiation program that causes a downregulation of P0 glycoprotein and Myelin Basic Protein (MBP),

marker of mature Schwann cells, and an up regulation of p75 neurotrophic Receptor (p75-NTR) and glial fibrillary acidic protein (GFAP), markers of immature Schwann cells.

These changes are accompanied by increased downstream of p38 and Erk1/2 mitogen-activated protein kinase (MAPK). Schwann cells response is also accompanied by activation of the ErbB2 receptor tyrosine kinase. This process is connected with nerve remodeling and regeneration. During nerve development, to regulate Schwann cells differentiation and myelination, ErbB2 receptor can be activated by axonal neuregulin, a growth factor expressed on axonal membrane (Wong KM et al., 2017).

All the described processes contribute to the damaged axon disruption and regeneration, but also to the modulation of nociceptors spontaneous activity and to their sensitivity to stimuli.

Also in DRG primary afferent cells bodies demonstrate maladaptive changes in their membrane composition, synapse structure, proprieties and location (Maecham K et al., 2017).

1.1.2 Central level

Central sensitization is defined as "Increased responsiveness of nociceptive neurons in the central nervous system to their normal or subthreshold afferent input". With repeated and/or intense stimulation spinal and cerebral pathways can become sensitized; if the persistent input is nociceptive, the sensitization becomes maladaptive (Gracely RH et al., 1992).

The increased responsiveness at the spinal cord level involves changes in calcium permeability, receptor overexpression, synapse location and glial activation. In supraspinal regions the main contributor to pain maintenance is the misbalance between descending facilitation and inhibition;

subcortical and cortical plasticity also contribute to painful interpretation of incoming signals (Maecham K et al., 2017).

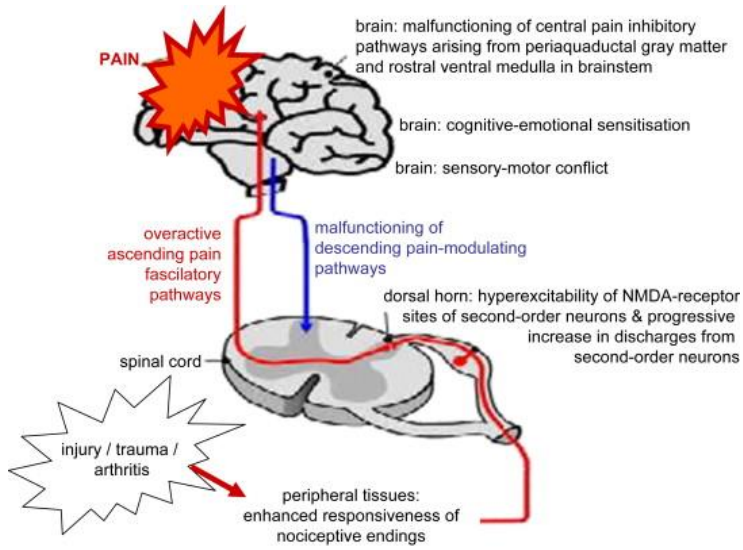

Figure 2. Peripheral and central nervous system activation following injury

The main increment in the spinal neuronal activity is attributable to the increased synaptic efficacy in the dorsal horns, at the second order neurons junction. Pain perception is dependent on glutamate action on AMPA receptors; in a chronic inflammatory state glutamate is continuously released together with substance P. After these neurotransmitters bind with their receptors, several protein kinases result activated, such as PKA, PKC, p38, MAPK etc. Moreover, ionotropic and metabotropic glutamate receptors are phosphorylated, increasing excitatory post-synaptic potential (EPSP), frequency and amplitude, which are further increased by alterations in glutamate homeostasis. Spinal cord neurons also alter channel expression levels to modify their proprieties. Also relevant is the activation of 5-HT_3 receptors, associated with pro-infiammatory cytokine release, and BDNF (Brain Derived Neurotrphic Factor) that acts on

microglia, enhances glutamate receptor phosphorylation and inhibits presynaptic inhibition by $GABA_a$ receptors, reducing the inhibitory tone (Maecham K et al., 2017). To date additional support is given also by the capability of neurons to transmit a signal in an antidromic manner. In abnormal situation, such as lesions and persistent pain, neurons are able to induce an action potential towards nociceptors, which release substance P, NGF and CGRP. These factors are pro-inflammatory and can lead to exacerbation of hyperalgesia as well as of peripheral inflammation (Willis WD ,1999).

In parallel with neuronal changes several modifications also take place in the other population present in CNS, glial cells. Upon activation, glia synthetize and release proinflammatory and pronociceptive mediators to enhance pain states, thanks to the activation of MAPKs pathways. The glia action has to be taken into account also because glial mediators can modulate synaptic transmission at lower concentrations than neurons (Suter MR et al., 2007).

Microglia are macrophage like cells that interact with synapse to modulate their structure and function for the CNS health. Hyperactivity of PNS nociceptive fibers causes the release of ATP and fractalkine that, binding on microglial receptors, lead to microgliosis. One of the main features of microgliosis are morphological changes; cells go from a ramified shape, useful to sense their environment in resting condition, to an amoeboid one when they are active. Beside morphological changes, microglia also undergo rapid proliferation. This spinal activation starts already two days after a lesion in mice models (Suter MR et al., 2007), peaking after a week, and slowly decreases during time.

Microglia activation by ATP induces BDNF release that in turn further increases ATP and glutamate release, giving rise to several processes such

as shielding injury sites, phagocytosing of cellular debris, and releasing inflammatory signals to initiate and/or propagate the immune response; microglial production of proinflammatory cytokines can further recruit microglia, promote sensitization and activate surrounding astrocytes.

Astrocytes are the most abundant cells in CNS. They display supporting action to neurons, actively interact with them through gap junctions, have contacts with synapses and blood vessels, have the ability to maintain K+ and glutamate homeostasis and control increase blood flow evoked by synaptic activity (Ji RR et al. 2013); this close contact permits to regulate external environment during synaptic transmission. Several lines of evidence demonstrate that astrocyte proliferation is a key process in induction and maintenance of neuropathic pain (Ji RR et al., 2013). Regarding the activation time course, microglia often precedes astrocytes activation and drives it through TNF-α release; astrocyte activation is thus more tardive compared to microglia and lasts longer. Active astrocytes release ATP that further acts on microglia, giving rise to a loop that supports the establishment of persistent pain.

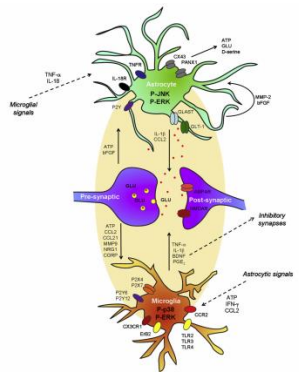

Figure 3. Neuronal-glial and glial-glial interaction (Ji et al., 2013)

Essential for the development of persistent pain is the activation of MAPKs in spinal cord glial cells; in fact, after the Ca++ flows into the cells consequent to the binding with glutamate, MAPK are phosphorylated and thus become active.

The MAPK family includes ERK1and 2, p38 and c-Jun N terminal Kinase (JNK).

In standard conditions, p38 is present at very low levels in glial cells, after inflammation its levels massively increase; indeed, p38 has been classified as stressed cells mediator.

Several lines of evidence have shown the increased phosphorylation of p38 (p-p38) after damage (Ji RR et al., 2013). The p38 is activated by ATP, TNF-α, IL-1β, CGRP; its activation induces synthesis and release of these mediators and prostaglandins that help transmit and reinforce pain signals; membrane receptors are also released , further facilitating pain perception **(**Ji RR & Suter MR, 2007).

1.2 Animal models of neuropathic pain

Neuropathic pain is extremely difficult to treat, given its complex etiology and its numerous manifestations**.** The pharmacotherapy has had limited success with commonly used pain reducing drugs, such as NSAIDS and opiates. There is therefore a considerable need to explore novel treatment modalities, and the best way to do so is the development of validated and reproducible animal models to test innovative therapies.

From 1970s, several animal models have been established to meet the diverse characteristics of the neuropathy, focusing on peripheral nerve

damages. The various available models differ for several features, such as the modality of pain induction (pharmacological or surgical), the gravity of the nerve lesion (compression, ligature or transection), the fibers involved (whole nerve or spared nerve) and time extent of pain manifestations (Jaggi AS et al., 2011). One of the most commonly employed models of chronic neuropathic pain is the Chronic Constriction Injury (CCI) of the rat sciatic nerve developed by Bennett and Xie. The constriction of the sciatic nerve is associated with intraneural edema, focal ischemia, and Wallerian degeneration. The behavioral phenotype mice display is characterized by guarding, excessive licking, limping of ipsilateral hind paw, avoidance of placing weight on the injury side and, sometimes, by mild to moderate autotomy. Changes observed are also mechanical and thermal hyperalgesia, chemical hyper-reactivity, cold allodynia and postural asymmetries. Electrophysiological studies also revealed the decrease in nerve conduction velocity (Jaggi AS et al., 2011).
In the present study the CCI has been performed according to procedure modified for mice, which is described in Materials and Methods section.

Chapter II: Nerve Growth Factor

Nerve Growth Factor (NGF) is a peptide synthetized and released by tissues during embryonic development promoting growth, differentiation and survival of neurons in central and peripheral nervous system. Since its discovery in 1950's by Levi-Montalcini and Cohen, other proteins with similar proprieties have been identified, Brain-Derived Neurotrophic Factor (BDNF), neurotrophin-3 (NT-3) and neurotrophin-4 (NT-4), which together are defined as neurotrophic factors, or neurotrophins.

NGF was described as a high molecular weight complex, denoted 7S NGF, containing three types of polypeptides (termed α, β and γ). Only the β subunit of the 7S complex has nerve growth promoting activity. βNGF is a dimer organized in two chains, each weighing 13,259 KDa and composed by 118 aminoacids. The chains are connected through three dysulfide bonds that give the protein a stable 3D structure. The mature form is derived from its precursor, proNGF, which beside the neurotrophic proprieties also displays pro-apoptotic features (Denk F et al, 2017).

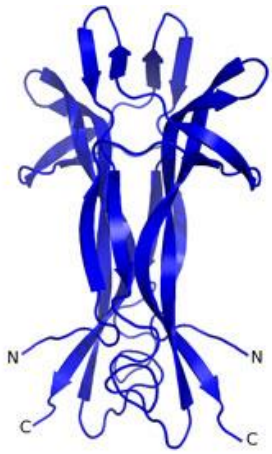

Figure4. Mouse NGF crystallographic structure (PBD: 1BET). Created with PyMol (www.pymol.org)

Along the years NGF has been object of several studies that demonstrated its presence at high levels in adult brain in hippocampus, cortex and olfactory regions (Korsching et al., 1985; Large et al., 1986), where it is important as neurotrophic factor for cholinergic basal neurons. Besides CNS, NGF is synthetized in several other cells, such as epithelial cells, fibroblasts, lymphocytes and mast cells (Gozes et al., 1983; Lindholm et al., 1987).

2.1 NGF receptors

Neurotrophins display their action binding to two classes of receptors: a common receptor, $p75^{NTR}$, which binds all neurotrophins with similar affinity, and a family of receptors, tyrosine kinases receptors (Trks) A, B and C, each of which is specific for a neurotrophin (Denk F et al, 2017).

The common neurotrophin receptor $p75^{NTR}$ is a member of the cysteine-rich-domain-containing receptors of the Tumour Necrosis Factor (TNF) receptor superfamily. $p75^{NTR}$ enhances the ability of Trk receptors to respond to neurotrophins and to discriminate for their preferred neurotrophin ligands (Bibel et al. 1999; Hempstead et al. 1991) . Under conditions of either reduced or absent Trk signalling, $p75^{NTR}$ promotes apoptosis following neurotrophin binding. In addition, $p75^{NTR}$ binds several other proteins with nanomolar affinities, including the neurotoxic prion protein fragment PrP and the Abamyloid peptide.

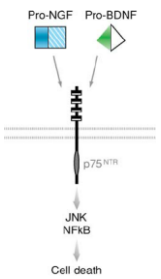

Figure5. $P75^{NTR}$ receptor. Pezet et al., 2006.

TrkA is the specific receptor that binds NGF (Huang & Reichardt 2003).

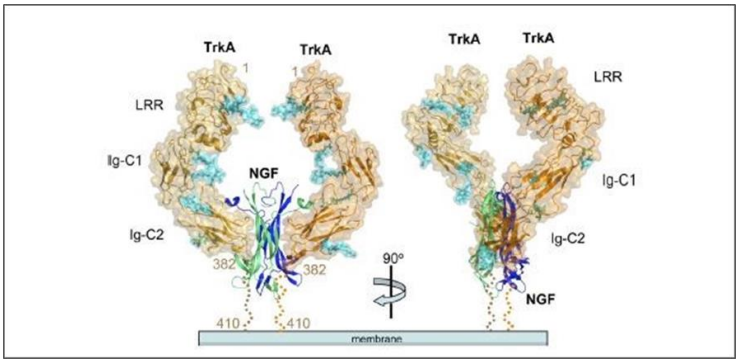

Figure6. TrkA structure and its binding with NGF. Wehman et al., 2007.

TrkA is expressed in various organs and tissues: central and peripheral nervous system, immune tissues, digestive tract, adrenal cortex, skin. TrkA receptor is also the main mediator of NGF-induced acute thermal hyperalgesia (Khodorova A et al., 2017).

TrkA is composed by one transmembrane structure, an extracellular domain that binds NGF and an intracellular domain with tyrosine kinase activity. Each NGF molecule binds two TrkA monomers, which result in dimerization and autophosphorilation of three tyrosines residues in the TrkA activation domain (Y670, Y674, and Y675). This enables the autophosphorylation of additional tyrosines, specifically Y490 and Y785.

This activated form of TrkA phosphorylates other intracellular matrix proteins including Shc, phospholipase Cγ (PLC-γ) and Src homology 2 domain-containing protein tyrosine phosphatase 2 (SHP-2), which then trigger the intracellular signal transduction system of NGF/TrkA

signaling, including the MAPK, phosphatidylinositol 3-kinase (PI3K) and PLC pathways.

The NGF–TrkA signalling complex is retrotransported in endosomes together with proteins of the p38 MAPK, ERK1, ERK2 and PI3K pathways along peripheral nerves to the cell bodies of nociceptive neurons in DRGs. This regulates the activity of several transcription factors, including c-FOS, c-JUN, ELK-1, forkhead-1, nuclear factor kappa B (NF-kB) and cAMP response-element-binding protein (CREB), which leads to alterations in expression of neuropeptides, channels and receptors.

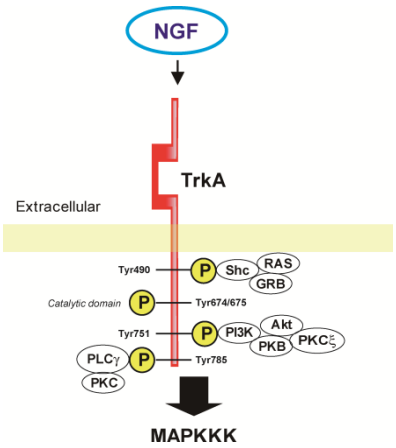

Figure7. Signal-transduction pathway of the TrkA tyrosine kinase receptor.
Adapted from Oda M et al., 2012.

2.2 NGF and pain

Besides its important role in nerve growth promotion, NGF is also known for its function in pain perception. Several evidences collected in the last decades in humans and animal models pointed out that NGF-mediated signaling is an active process in chronic pain condition, and helped understand the mechanism of action through which the process occurs.

2.2.1 Mechanism of action

One of the first events after injury or inflammation of tissues is the release of proinflammatory cytokines that triggers the release of NGF, which contributes in several ways to acute and chronic inflammatory processes.

NGF may act directly on nociceptive neurons, acting on the transient receptor potential vanilloid receptor 1 (TRPV1). TRPV1 is a cation channel and is the capsaicin receptor. It is expressed on nociceptors and is a molecular detector of dangerous heat and acidification, which occurs during inflammation. When TRPV1 is activated leads to the influx of Ca^{++} that, in turn, leads to membrane depolarization and thus to action potential. NGF potentiates TRPV1 channels through CaMK and PKC acting downstream on PI3K, which sensitizes TRPV1 by direct phosphorylation, which leads to increased channel activity and translocation of the channel to the cell surface (Hefti FF et al., 2006; Norman BH & McDermott JS 2017).

Retrograde NGF signaling modulates and increases the expression of several proteins that further sensitize neurons as well as a variety of

receptors. These receptors are involved in nociception and include bradykinin receptors, acid-sensing ion channels (ASIC) 2/3, voltage-gated sodium channels, voltage-gated calcium channels, as well as the already mentioned TRPV1 that from the cell bodies are transported to the terminals (Chang DS et al., 2016). Other modulated proteins are substance P, BDNF and CGRP that facilitate activation of second-order neurons in the CNS (Hefti FF et al., 2006).

A further effect of NGF in the pain process is exerted through its binding on TrkA on Mast cells; NGF is in fact a key regulator of the cross-talk between the immune and nervous system (Minnone G et al., 2017). Mast cells are part of the immune system; they were first known for their role in allergies and later their role in several other processes has been discovered. They are involved in innate or acquired immunity, bacterial infections, autoimmunity. They are also critical for the pathogenesis of inflammatory diseases, such as arthritis, atopic dermatitis, psoriasis, and multiple sclerosis (Theoharides TC et al., 2012).
After NGF binding, through a process known as “degranulation”, several inflammatory mediators are released, such as histamine, prostaglandins, 5-HT and NGF itself, giving rise to a positive feedback loop (Hefti FF et al., 2006).

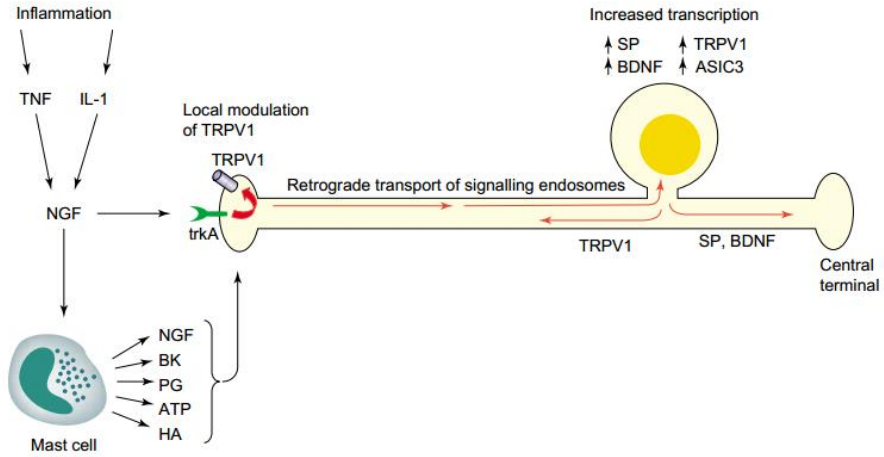

Figure8. NGF action after inflammation. Hefti et al., 2006

It is thus noticeable that NGF not only directly increases the action and expression of peripheral nociceptive receptors and pro-nociceptive neurotransmitters, but also indirectly synthetizes adjacent nociceptive neurons in response to inflammation.

2.2.2 Evidence: basic science and clinics

The described mechanisms through which NGF is involved in pain perception and maintenance arise from years of evidence collected in human symptomatology and animal models.

One of the studies that disclosed the NGF relation with pain demonstrated that NGF administration in healthy subjects was able to induce allodynia, tenderness and hypersensitivity on the site of injection (Dyck PJ et al., 1997); muscle pain and hyperalgesia, lasting for more than a week after NGF treatment, were also observed (Svensson P et al., 2003). Similar results were found in animal models. Local and systemic NGF administration in mice result in robust and long lasting mechanical and thermal hyperalgesia (Lewin GR et al., 1994); NGF injection into rat

tibia activates and sensitizes bone nociceptors and produces acute behavioral response (Nencini S et al., 2017).

Moreover, intrathecal NGF administration induces sprouting of peripheral nociceptive fibers, leading to hyperalgesic state (Pertens E et al., 1999).

An in vitro experiment demonstrated that neuronal culture treated with NGF results to have increased ASIC3 expression that can account for neuronal hyperexcitability and hyperalgesia (Mamet J et al., 2003).

Beside the direct painful effects of its injection, indirect evidence of NGF involvement in pain has been shown. In fact, enhanced NGF levels were initially found in the cerebrospinal fluid of multiple sclerosis patients, and it was shown that an increase in NGF closely follows the course of the disease (Bracci-Laudiero L et al., 1992). The synovial fluids of patients with rheumatoid arthritis and spondiloarthritis (Aloe L et al., 1992; Barthel C et al. 2009) are also characterized by an increased concentration of NGF. Moreover, Systemic Lupus Erythematosus (SLE) patients exhibit a significant increase in NGF concentration in the sera (Bracci-Laudiero L et al., 1992; Aalto K et al., 2002), increase that correlates with disease activity.

In mice models too the NGF concentration increases in several tissues, e.g. in skin after injection of irritants (Hetfi FF et al., 2006), in synovia of mice models of induced arthritis (Manni L et al., 1998), in sera of mice model of SLE (Bracci-Laudiero L et al., 1996) and in epithelial cells of inflamed colon (Stanzel RD et al., 2008).

Another important evidence of relevance of NGF system in pain perception lies in a genetic syndrome in humans.

In fact, mutations of the NTRK1gene, coding for TrkA and of the NGFB gene lead to the development of rare forms of congenital insensitivity to

pain HSAN IV (human sensory and autonomic neuropathy type) (OMIM #256800) and HSAN V (OMIM #608654), respectively.
Both syndromes are characterized by severe pain insensitivity, but differ as HSAN IV patients show also anhydrosis and mental retardation, while HSAN V patients show no other neurological and cognitive deficits (Capsoni S et al., 2011).

2.3 NGF/TrkA pathways: development of analgesics

Since NGF/TrkA system is a master control system for pain, lots of effort has been made through the years to develop compounds that inhibit the signaling to reduce pain.
Analgesic effects have been obtained through the inhibition of TrkA activity. It is in fact possible to create drugs that penetrate the cell membrane and, having an amino acid sequence partially equivalent to TrkA's, block the activation loop substituting the receptor itself (Hirose M et al., 2008).

However, the vast majority of the studies have focused on the blockade of the pathway using antibodies, which have the merit to be highly specific and to have reduced off target effects.
There are two possible ways of blocking the signaling, acting on the receptors or on the NGF itself.

Considering the receptor, just one monoclonal antibody anti-TrkA, MNAC13, has been developed, MNAC13 by Catteneo et al. (1999, Patent

n. AU2006256387, 2011; EP1893649, 2012; AU2006260490, 2011; US7988966, 2011), then licensed to Glenmark Pharmaceuticals, a pharmaceutical company, that is currently developing another antibody, BXL1H5, derived from MNAC13 and reported to be completing phase 1 testing.
MNAC13 is proven to induces analgesia in murine models of chronic and inflammatory pain (Ugolini G et al., 2007) and reduces pain after bone fracture (Rapp A et al., 2015).

Focusing on NGF instead, several antibodies have been developed, they act capturing NGF and their efficacy has been demonstrated in various animal models.
They result in fact to be able to prevent the pain status in models of inflammatory and visceral pain (Woolf CJ et al., 1994; Lamb K et al., 2003). It is also demonstrated that they can reduce established hyperalgesia in arthritis (Shelton DL et al., 2005) and hypersensitivity in bone cancer models (Sevcik MA et al., 2005).
Clinical trials using humanized anti-NGF, such as Tanezumab (Pfizer), Fulranumab (Amgen/Janssen), PG-110 (Abbott), MEDI578 (Medimmune) and REGN475 (Regeneron/Sanofi) have been conducted for the treatment of neuropathic pain and osteoarthritis, but because of safety issues have been suspended and further need of preclinical studies has emerged.

Others experiments have focused on low affinity receptor $p75^{NTR}$ to try to obtain analgesic effects as well. Fukui et al. (Fukui Y et al., 2010) demonstrated that anti-$p75^{NTR}$ polyclonal antibody has antihyperalgesic effect in a mouse model of neuropathic pain and also prevents the

establishment of inflammatory pain induced by carrageenan (Watanabe T et al., 2008), NGF and pro-NGF (Khodorova A et al., 2013).

We focused on two monoclonal antibodies, MNAC13 and αD11, as well as the new $p75^{NTR}$-Fc to further investigate their effects and proprieties.

2.3.1 MNAC13

Mouse monoclonal MNAC13 is the only anti-TrkA humanized antibody currently under pre-clinical development. It specifically binds receptor extracelluar domain and leads to inhibition of NGF-dependent signaling preventing TrkA from being activated by NGF. Its structure and function have been well characterized (Cattaneo A et al., 1999; Covaceuszach S et al., 2005) and its analgesic power has been investigated by Ugolini et al. in two different pain models. These authors demonstrated that in a murine neuropathic pain model, repeated injections of MNAC13 (70μg/mouse/8 days) was able to induce long lasting antihyperalgesic effects, moreover it was able to potentiate the analgesic effects of opiates and to prevent the onset of pain in inflammatory mouse model after formalin injection (Ugolini G et al., 2007).

2.3.2 αD11

Cattaneo group developed in 1988 αD11 (Cattaneo A et al., 1988, patent no. NZ564071 (A) 2005; EP1893649, 2012; AU2006260490, 2011; US7988966 , 2011). It is a rat monoclonal antibody that directly binds and captures NGF.binds mouse NGF with picomolar affinity with no cross-reactivity towards other neurotrophins; αD11 antagonizes very effectively the NGF biological function in a variety of in vitro and in vivo

systems. In order to be suitable for human trials αD11 has been humanized (Covaceuszach S et al., 2004). After being tested in vitro and in vivo, it has been demonstrated that mAbαD11 binds equally well to human and mouse NGF, showing that the binding mode and the NGF neutralizing biological activities were fully preserved (Covaceuszach S et al 2012). Covaceuszach et al. also evaluated in vivo the analgesic potential of the compound. They demonstrated that αD11 was able to prevent the inflammatory pain derived from formalin injection, and that eight administrations of 70μg/mouse of the mAb had long lasting antihyperalgesic effects on a neuropathic pain model.

2.3.3 $p75^{NTR}$-Fc

Recently, Levicept Ltd., a biotechnology company, had a patent assigned following the closure of Pfizer Sandwich on the "USE OF P75NTR NEUROTROPHIN BINDING PROTEIN" (Composition of matter patent PC71902 Inventor: Simon Westbrook).

Levicept's focus is the discovery and development of novel biological therapies for the treatment of pain. Levicept is currently developing the novel neurotrophic scavenging molecule p75-Fc, for the treatment of neuropathic and inflammatory pain.

$p75^{NTR}$-Fc is soluble form of p75NTR fused with an Fc fragment that partially binds nerve growth factor (NGF) and other neurotrophins and acts as NGF scavenger. Exploring its proprieties is interesting since $p75^{NTR}$-Fc might provide analgesia while maintaining high the neurotrophin level. As a matter of fact, $p75^{NTR}$-Fc treatment maintains neurotrophin homeostasis by providing stable binding proteins for the excess neurotrophins present in chronic pain states.

In pre-clinical models of osteoarthritis, administration of $p75^{NTR}$-Fc provides analgesia equivalent to that achieved with anti-NGF antibody treatment (LEV003-2, Levicept ltd, Simon Westbrook).

$p75^{NTR}$-Fc is actually on clinical trials; it is being developed as a once-a-month injectable for the treatment of osteoarthritis and chronic pain.

Chapter III: Experimental design

3.1 Aim of the project

Chronic pain is a condition that affects 20% of the population and the number tends to increase as population age. Among these patients it is difficult to identify the prevalence of neuropathic pain, since it is often secondary to several diseases, such as diabetes, stroke, multiple sclerosis and spinal cord injury, for example.

It is anyhow clear that neuropathic pain is a disabling state that affects a large part of the population and has a huge impact on quality of life. It reflects on physical and psychological health, since depression, anxiety, and sleep disorders are significantly more prevalent in patients with NP compared to those without such pain. NP also has an important impact on daily activities, employment and economic status, reflecting on loss of work productivity. An important consequence is also the rise of health care costs, estimated at € 300 billion in EU annually and $ 600 billion in US (Bonakdar RA, 2017).

Current treatments include NSAID's, opioids, antidepressants and anti-convulsants, but the outcome are not always satisfactory; patients achieve partial relief, some of them become resistant to drugs and suffer from severe side effects.

It is therefore important to develop novel therapeutic strategies.

Recently the NGF/TrkA pathway has strongly emerged as a target for neuropathic pain, given its regulatory role in pain. Several lines of evidence have been collected of the efficacy of anti-NGF antibodies in preclinical models. In clinical trials the analgesic effects were confirmed,

but safety concerns have risen, highlighting the need of going back to preclinical.

For this reason, we decided to investigate the anti-hyperalgesic potential of blocking NGF/TrkA signaling, acting on all its components: the neurotrophin, using the anti-NGF αD11, the receptor, using MNAC13, the only anti-TrkA humanized monoclonal antibody available, as well as a novel NGF scavenger, $p75^{NTR}$-Fc.

In murine models the three compounds have already demonstrated their effectiveness. MNAC13 and αD11 are able to reduce neuropathic pain and prevent inflammatory pain, while $p75^{NTR}$-Fc is able to counteract osteoarthritis.

The focus of the present study was to evaluate if the effect of MNAC13 and αD11 on neuropathic pain would last longer than previously demonstrated and if any structural and morphological alteration was induced in central and peripheral nervous system. We also wanted to verify if $p75^{NTR}$-Fc was able to induce analgesia also in our neuropathic pain model, in addition to the already demonstrated effects on osteoarthritis.

To achieve our purpose we took advantage of the model of neuropathic pain induced by CCI of the sciatic nerve. On this model we tested the efficacy of the compounds to reduce mechanical allodynia. Both the mAbs showed a very long lasting analgesic effect, which was not present after the administration of the scavenger.

To understand how these behavioral changes reflected on the nervous system, we performed immunohistochemical analysis on the sciatic nerve and spinal cord dorsal horns, ipsilateral to the ligature. We analyzed the expression of glial and neuronal markers associated with inflammation, neurodegeneration and regeneration.

To better understand the mechanism underling the behavioral, morphological and functional changes driven by MNAC13 and αD11, we performed an ELISA on mouse serum samples to evaluate pharmacokinetics of the antibodies, and an immunoprecipitation in brains of treated mice to clarify if the mAbs were able to cross the Blood-Brain Barrier. The outcome of these experiments is critical, since they allow to speculate about the mechanism of action of the compounds, and to have data on the safety of the treatments.

Our final goal is to provide new information that will hopefully help develop more effective end safe analgesic drugs, which will permit patients to better deal with their condition.

3.2 Materials & methods

3.2.1 Animals

Male C57BL/6J mice were purchased from Charles River (Wilmington, Massachusetts, USA), housed 4 per cage with food and water ad libidum and maintained on a 12:12-h dark:light cycle (lights on from 7 AM to 7 PM). After two weeks, at three months of age, they underwent surgery and were randomly assigned to the different experimental groups. All procedures were approved by the ethic committee of the Italian Ministry of Health and conducted under license/approval ID #: 21-2014 PR, according to the Italian national law (D. Lgs. 26/14) and the European Communities Council Directive (2010/63/EEC) on the use of animals for experimental research.

3.2.2 Surgery

The CCI model was used as model of neuropathic pain, adapting to mouse the original Bennett and Xie procedure (Bennett and Xie 1988). Mice were anesthetized with Ketavet (Ketamina e Xilazina 0.02 g/Kg), an incision of about 1,5 cm was made on the right hindlimb to expose the sciatic nerve. Three ligatures were performed (ETHICON PROLENE 7-0) 1mm from each other (fig.8).

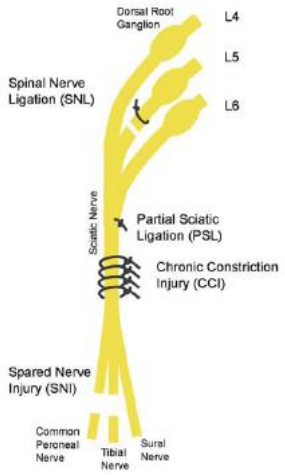

Figure9. Sciatic nerve ligature (Campbell & Mayer 2016)

The wound was then closed (Ethicon Vicryl 4-0). The animals were left to recovery 3 days before the beginning of the experiments. The CCI procedure causes the development of neuropathy characterized by mechanical allodynia (pain due to a mechanical stimulus that does not normally provoke pain) in the paw ipsilateral to the ligature. This feature has been used to evaluate the analgesic power of the compounds (Luvisetto S et al., 2007).

3.2.3 Treatments

The compounds used were:

-anti-TrkA mAb MNAC13 (Ugolini G et al. 2007)

-anti-NGF mAb αD11 (Covaceuszach S et al. 2012)

-p75NTR-Fc (Levicept, patent WO 2013136078 A1)

According to the experimental group they were assigned to, mice were intraperitoneally (i.p.) injected from D3 to D10 with the compounds, diluted in saline (0,9%), at different doses. Control groups were injected with saline.

We performed different experiments. In the first one we tested two groups of mice:

-group 1: composed by 8 mice treated with 70µg/mouse/day MNAC13

-group 2: composed by 10 mice treated with 70µg/mouse/day αD11

In the second experiment we raised the dose to evaluate if the effect would have been prolonged, and we tested:

-group 3: composed by 10 mice treated with 100µg/mouse/day MNAC13

-group 4: composed by 10 mice treated with 100µg/mouse/day αD11

We performed behavioral assay also with $p75^{NTR}$-Fc, which provides stable binding proteins for the neurotrophins excess present in chronic pain states, and we evaluated the mechanical threshold of:

-group 5: composed by 10 mice treated with 90µg/mouse/day $p75^{NTR}$-Fc.

Each treated group had its own saline treated control group. Since the effect of the lowest dose of MNAC13 and αD11 disappeared after a month, all the molecular analysis have been performed on tissues from mice that received the highest dose of 100µg/8 days of the mAbs.

3.2.4 Mechanical nociceptive threshold (Dynamic plantar aesthesiometer test)

The development of neuropathy was assessed measuring the sensitivity of both hindpaws, ipsi and contralateral to the ligature. For the measurement we used Dynamic Plantar Aesthesiometer (Ugo Basile, Model 37400), an apparatus that applies a punctuate stimulus with a linear growing force. The stimulus is applied on the plantar surface of the paw and, when the mouse withdraws it, the force in grams applied defines the nociceptive threshold. Mechanical allodynia is developed when a stimulus usually not painful becomes noxious, and thus mice lift the ipsilateral paw at a lower force than the contralateral one. Test begins 3 days after CCI; mice were left to habituate to the apparatus (fig.10) for 10 minutes before being tested.

Figure10. Dynamic Plantar Aestesiomether

The mechanical withdrawal response of ipsilateral and contralateral hindpaws was recorded for 3 consecutive trials with at least 10 seconds between each trial. The withdrawal threshold assessed was obtained from the mean of the 3 trials (Luvisetto S et al., 2007). The increase of the force borne by the paw ipsilateral to the ligature was used as a

measure of the efficacy of the tested compounds, leading ipsilateral score closer to contralateral.

3.2.5 Immunohistochemistry

For immunohistochemical analysis, ligated sciatic nerve and lumbar spinal cord (SC, L4-L5) of mice belonging to each experimental group (saline, MNAC13 and αD11, n = 3/group) were collected at different time points (NAÏVE, D3, D11, D24, D90). Animals were given a sub-lethal dose of Ketavet and were then perfused with saline followed by 4% paraformaldehyde in phosphate buffer saline (PBS, pH 7.4). Sciatic nerve and SC were removed and kept in immersion for 48 h in 4% paraformaldehyde PBS, then 24 h in cryoprotection with solution of 30% (w/v) sucrose in PBS and stored at −80 °C until use. Cryostat sections were taken, 25 μm for sciatic nerve and 40 μm for spinal cord.

For sciatic nerve the sections obtained were incubated overnight with primary antibodies, while for SC the sections were incubated for 48h (see Table1). After three washes with PBS tissues sections were incubated for 2 h at room temperature with secondary antibodies. All antibodies were diluted in Triton 0,3% (Sigma-Aldrich). After two washings in PBS, sections were incubated for 10 minutes with bisBenzimide, DNA-fluorochrome (Hoechst, 1:1000, Sigma-Aldrich) in PBS

Sciatic nerve			
Name	Informations	Diluition	Use
anti-S100β	mouse monoclonal, S2532; Sigma-Aldrich	1:200	Schwann cells marker
Neu200	rabbit polyclonal, N4142; Sigma-Aldrich	1:200	Nurofilament marker
P0/MPZ	chicken polyclonal, AB9352; Millipore	1:200	Myelin protein zero marker
CC1	mouse monoclonal, SC-59586; Santa Cruz Biotechnology	1:200	Mast cells chymase marker
Spinal cord			
Name	Informations	Diluition	Use
anti-GFAP	mouse monoclonal, G6171; Sigma-Aldrich	1:200	Glial Fibrillary Acidic Protein, astrocytes marker
Anti-p-p38	rabbit polyclonal, sc-28533; Santa Cruz Biotechnology	1:200	Phosphorilated MAPk, cell activation marker
IBA1/AIF1	chicken polyclonal, No. 234 006; Synaptic Systems	1:400	Ionized calcium-Binding Adaptor molecule1, microglia marker

Table1. Primary antibodies used for immunohistochemistry

Secondary antibodies			
name	Informations	Diluition	Color
Alexa Fluor 488	fluorescein-conjugated donkey anti-mouse; Jackson ImmunoResearch	1:200	Green
FITCH	fluorescein-conjugated goat anti-rabbit; Santa Cruz Biotechnology	1:200	Green
TRITC	rhodamine conjugated goat anti-rabbit; Jackson ImmunoResearch	1:200	Red
Cy3	Cy3-conjugated donkey anti-chicken; Jackson ImmunoResearch	1:200	Red
Alexa Fluor 647	rhodamine 647 conjugated donkey anti-rabbit; Jackson ImmunoResearch	1:200	Blue

Table2. Secondary antibodies used for immunohistochemistry

All images were acquired by laser scanning confocal microscopy using a TCS SP5 microscope (Leica Microsystem) connected to digital camera diagnostic instruments operated by I.A.S. software of Delta Systems Italia. Figures were assembled by using Adobe Photoshop CS3 and Adobe Illustrator 10. Quantification was performed by using the ImageJ software (version 1.41, National Institutes of Health, USA).

For sciatic nerve analysis high (63X) magnification images of immunostained sections were acquired. The fluorescence of all different markers was quantified with RGB (Red, Green and Blue) method (Inman CF et al., 2005). The number of pixels of each color was

automatically counted and then converted to a brightness value, using ImageJ software (http://rsb.info.nih.gov/ij/). The number of positive immunoreactive (IR) cells was automatically counted (three sections/animal) with a mark and count tool and for each experimental group the mean of three animals was calculated (Cobianchi S et al., 2010, Marinelli S et al., 2010, Inman CF et al., 2005).

For SC low (10X) and high (63X) magnification images of immunostained sections were acquired. To quantify the immunoreactivity of astrocytes and microglia, high magnification images of the ipsilateral side of the dorsal horns (laminae I-IV) for each animal were captured with a 63X objective at zoom factor 1 by using a constant set of acquisition parameters.

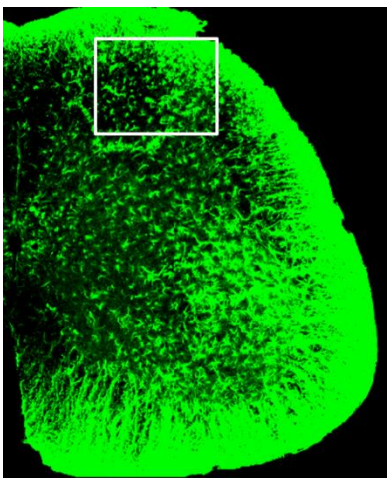

Figure 11. Representative 10x image stained for GFAP. The rectangle indicates the area analyzed, dorsal horns (laminae I-IV) ipsilateral to the ligature.

For analysis of labelling, the entire image (a square of 230 μm of side) of the ipsilateral side of spinal cord was quantified by counting number of IR cells and colocalization with p-p38. The RGB (red, green, blue) analysis, which converts RGB pixels to brightness value, was also used to evaluate the markers' fluorescence. Three images were used for each animal and for each experimental group the mean of three animals was calculated (Vacca V et al., 2016).

3.2.6 ELISA

To evaluate the levels of circulating antibodies in the bloodstream, we collected serum samples from mice at different time points (D11, D24, D46, D72, D90) and performed two ELISA assay.

Mice treated with MNAC13 or αD11 and with saline for 8 days (n=5 per group) were sacrificed by decapitation, blood samples were kept 30 min at room temperature and centrifuged 15 min at 300 rpm. Serum was collected and maintained at -80° until use.

In the ELISA for MNAC13 PK, the Recombinant human TrkA Fc Chimera R&D was used as capture antibody. The calibration curve was carried out using purified MNAC13 (range: 2-0.031 ng/ml, serial dilution in milk, 1:2, duplicates). The samples were checked at least at three different dilutions, both neat and MNAC13 spiked. Samples and curve were incubated 2 hours at room temperature. The MNAC13 antibody was detected by using a HRP conjugated anti-mouse IgG (Minimum Cross Reactions, Jackson laboratories), incubated 1 hour at room temperature.

In the ELISA for αD11 PK, recombinant human NGF (produced by EBRI) was used as capture protein. The calibration curve was carried out using purified αD11 (range: 2-0.031 ng/ml, serial dilution 1:2 in milk,

duplicates). The samples were checked at least at three different dilutions, both neat and αD11 spiked. Samples and curve were incubated 2 hours at room temperature. The αD11 antibody was detected by using a HRP conjugated anti-rat IgG (Minimum Cross Reactions, Jackson laboratories), incubated 1 hour at room temperature.

3.2.7 Immunoprecipitation

To evaluate if the mAbs were able to pass through the Blood Brain Barrier we performed an Immunoprecipitation assay. The first step of our experiment was to incorporate UV-traceable biotin onto anti-TrkA and anti-NGF, as described in the product data sheet (ChromaLink Biotin, DMF Soluble; SoluLink,San Diego, CA, USA). The compounds were then ip administered in mice assigned to the following groups:

-MNAC13 treated: n.2 CCI and n.2 naïve mice ip injected with biotinylated MNAC13 100µg/mouse/day for 8 days

- αD11 treated: n.2 CCI and n.2 naïve mice ip injected with biotinylated αD11 100µg/mouse/day for 8 days

-control: n.2 CCI and n.2 naïve mice ip injected with saline for 8 days

Mice were given a sub-lethal dose of Ketavet and were perfused with saline to avoid the possibility of blood interference in the process. Brains were then removed, immediately frozen in liquid nitrogen and stored at -80° until use.

Immunoprecipitation was performed using resin conjugated with streptavidin (Streptavidin Agarose Ultraperformance, SoluLink, San

Diego, CA, USA). Brains were lysed and 15mg of total proteins were loaded on the streptavidin. The streptavidin strongly binds with the biotin, making possible to detect even small amount of marked antibody. Positive controls were loaded (MNAC13 mAb and αD11 mAb) in addition to samples.

Samples were ran in SDS page and then blotted on nitrocellulose membrane.

After overnight blocking with milk, the membrane was incubated with secondary antibodies. The MNAC13 antibody was detected by using a HRP conjugated anti-mouse IgG (Minimum Cross Reactions, Jackson laboratories. 1:4000 in Milk 5% in PBS-Tween 0.025%; 3 h incubation r.t.), αD11 antibody was detected by using a HRP conjugated anti-rat IgG (Minimum Cross Reactions, Jackson laboratories. 1:4000 in Milk 5% in PBS-Tween 0.025%; 3 h incubation r.t.).

3.3 Statistics

All values are expressed as mean ± SEM. Two-way ANOVAs for repeated measures were used to analyze the effects of treatment; when necessary, post hoc comparisons were carried out using Tukey-Kramer test. The statistical analysis of immunohistochemical data and ELISA assay were carried out by t-test. Differences were considered significant at $p < 0.05$.

Chapter IV: Results

4.1 Mechanical nociceptive threshold

The CCI procedure induces mechanical allodynia in all experimental groups, demonstrated by the reduction of the withdrawal mechanical threshold of the ipsilateral paw.

In the first experiment we administered mice with 70µg/day of MNAC13 and αD11. Mice show an increase of the withdrawal threshold compared to saline treated group with onset at D7 and D10, respectively. These analgesic effects are maintained for approximately a month, specifically D19 for MNAC13 (fig.12) and D31 for αD11 (fig.13).

Statistical analysis for the different groups revealed:
- group 1, MNAC13 : significant effect of treatment ($F_{1,14}$=19,698; p<.001), time ($F_{22,308}$=10, 076; p<.001), and a significant interaction between time and treatment ($F_{22,308}$=3,83; p<.001). Post hoc analysis showed significant difference from D7 to D19, except for D17.

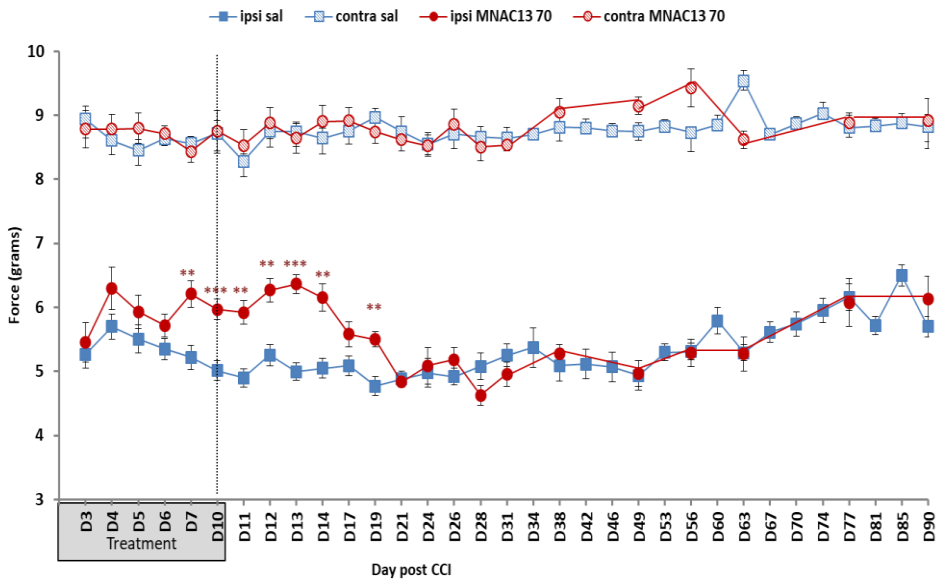

Figure12. Temporal trend of mechanical allodynia recorded in ipsilateral (ipsi) hindpaws. In red is represented the group treated with 70µg/day of **MNAC13**, in blue the controls injected with saline (sal). Symbols with lighter colors refer to contralateral (contra) values. Values are expressed as means±SE.*p<.05, **p<.01, ***p<.001.

- group 2: significant effect of treatment ($F_{1,18}$=33,797; p<.001), time ($F_{32,576}$=4,426; p<.001) and a significant interaction between time and treatment ($F_{32,576}$=5,303 p<.001). Post hoc analysis showed significant difference from D10 to D31.

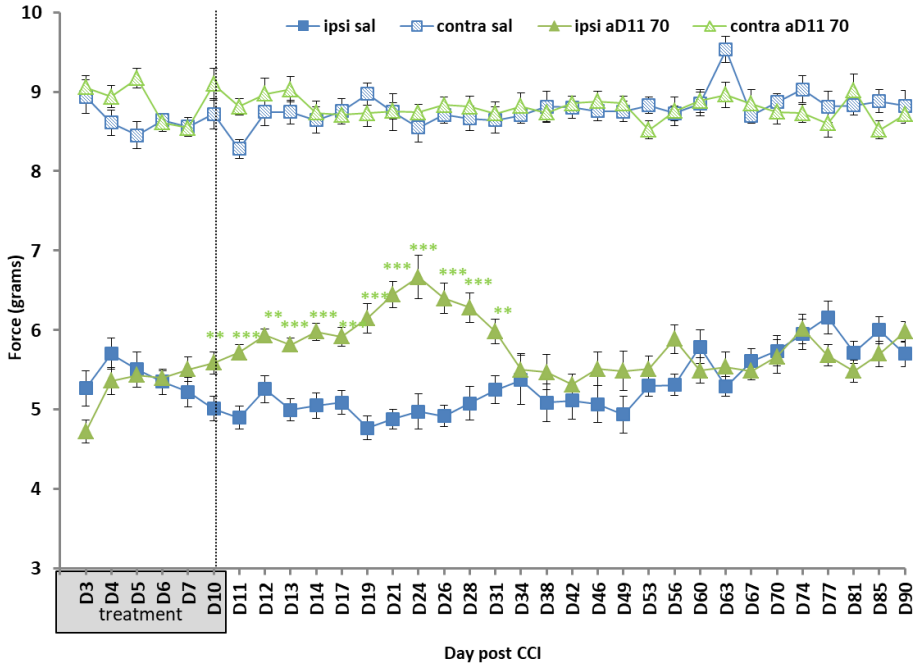

Figure13. Temporal trend of mechanical allodynia recorded in ipsilateral (ipsi) hindpaws. In green is represented the group treated with 70µg/day of **αD11,** in blue the controls injected with saline (sal). Symbols with lighter colors refer to contralateral (contra) values. Values are expressed as means±SE.*p<.05, **p<.01, ***p<.001.

In the second experiment, given the promising results already obtained, we increased the dose, reaching 100µg/mouse/day. The behavioral tests showed that, at the higher dose, both mAbs maintained their antiallodynic effects much longer, for 90 days after the administration (fig.14 and 15 show long lasting effects of MNAC13 and αD11 respectively).

- group 3: significant effect of treatment ($F_{1,18}$=79,996 p<.001), time ($F_{32,576}$=9,676 p<.001) and of their interaction ($F_{32,576}$=8,637, p<.001). Post hoc analysis showed significant differences from D7 to D90.

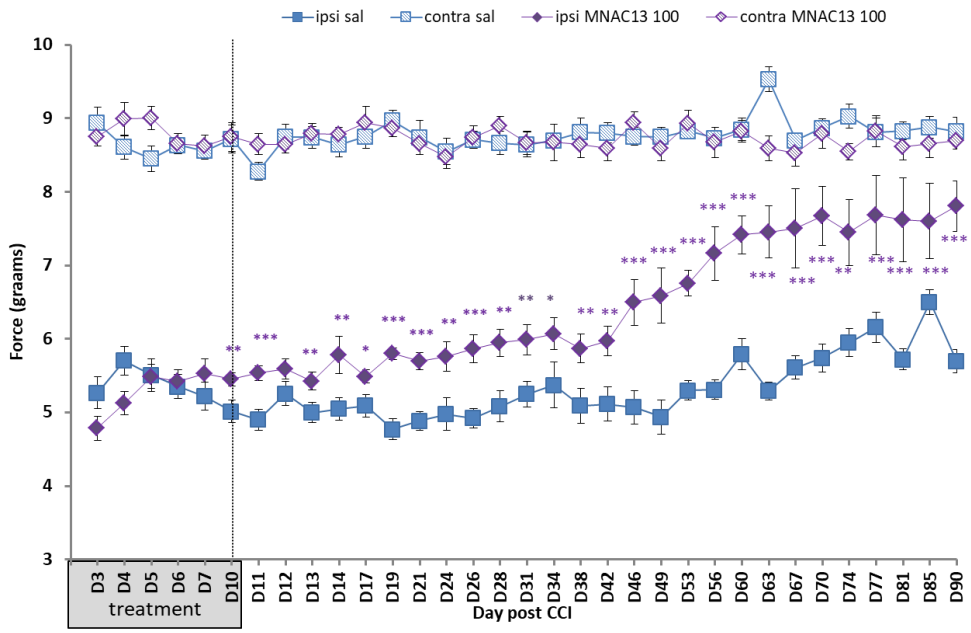

Figure14. Temporal trend of mechanical allodynia recorded in ipsilateral (ipsi) hindpaws. In violet is represented the group treated with 100µg/day of **MNAC13** in blue the controls injected with saline (sal). Symbols with lighter colors refer to contralateral (contra) values. Values are expressed as means±SE.*p<.05, **p<.01, ***p<.001.

-group 4: significant effect of treatment ($F_{1,18}$=345,077 p<.001), time ($F_{32,576}$=5,656 p<.001) and a significant interaction between time and treatment ($F_{32,576}$=7,589; p<.001). Post hoc analysis showed significant differences from D14 to D90.

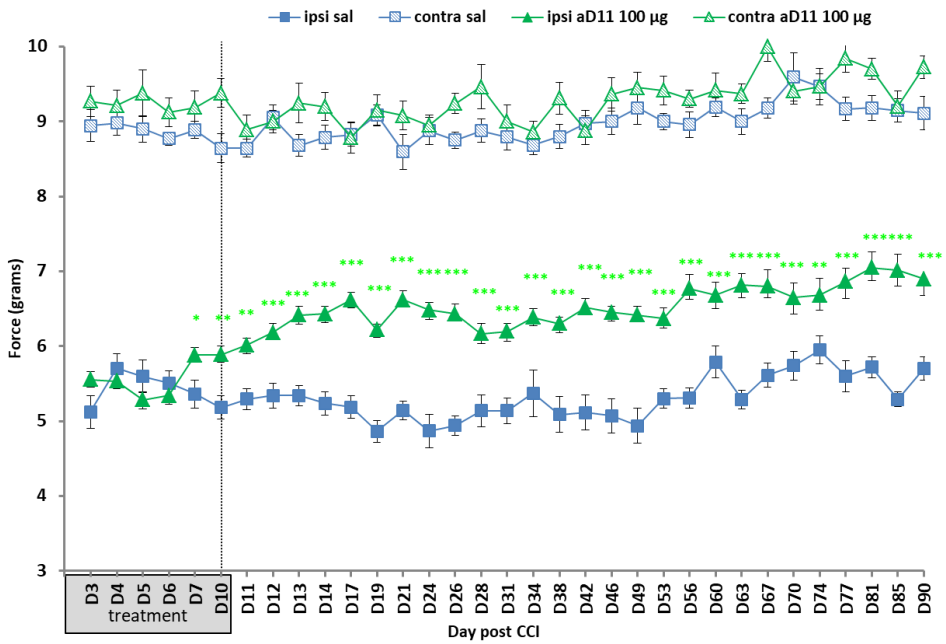

Figure15. Temporal trend of mechanical allodynia recorded in ipsilateral (ipsi) hindpaws. In green is represented the group treated with 100µg/day of **αD11**, in blue the controls injected with saline (sal). Symbols with lighter colors refer to contralateral (contra) values. Values are expressed as means±SE.*p<.05, **p<.01, ***p<.001.

At this point we decided to investigate if the analgesic effects of MNAC13 would be maintained longer than 3 months, and when they would disappear. Thus, we tested a new group of mice treated with antiTrkA until D150. As far as the temporal trend of the analgesic effects of MNAC13 is concerned, nociceptive thresholds of treated mice were significantly higher than those obtained by control group until D130, significant differences that disappeared at D140 and D150 (fig.16)

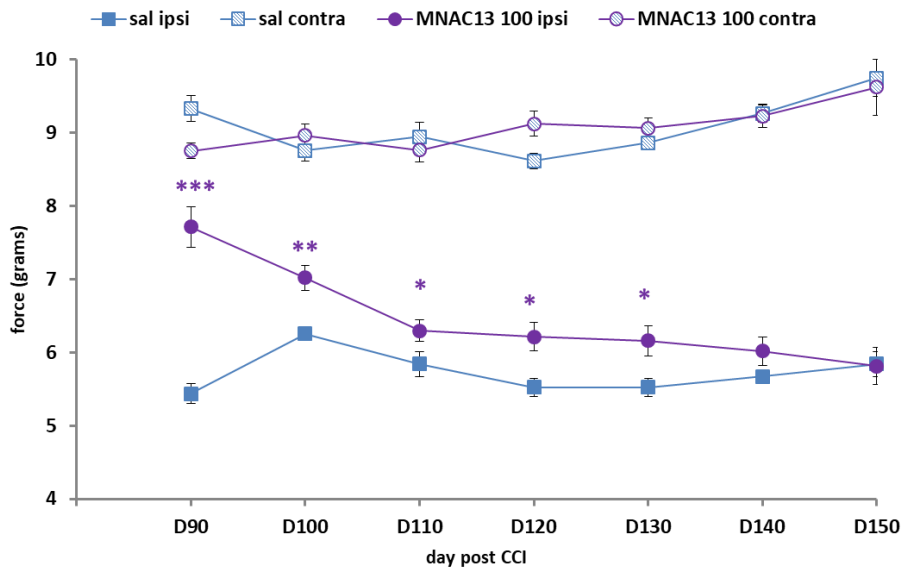

.

Figure16. Temporal trend of mechanical allodynia from D90 to D150 recorded in ipsilateral (ipsi) hindpaws. In violet is represented the group treated with 100µg/day of MNAC13, in blue the controls injected with saline (sal). Symbols with lighter colors refer to contralateral (contra) values. Values are expressed as means±SE.*p<.05, **p<.01, ***p<.001.

MNAC13 and αD11 at the highest dose induce a significant increase in the mechanical threshold, indicating a strong antiallodynic effect, which was maintained for long after the end of the treatment. A complete recovery from the neuropathic condition is, however, not present: the difference between mechanical thresholds of ipsi and contralateral paws is statistically significant for both treated groups (paw: MNAC13 $F_{(1,18)}$=250,383, p<.001; αD11 $F_{(1,18)}$=993,242, p<.001; time: MNAC13 $F_{(18,32)}$=8,382, p<.001; αD11 $F_{(18,32)}$=4,734, p<.001; interaction MNAC13 $F_{(18,32)}$=8,135, p<.001; αD11 $F_{(18,32)}$=2,982, p<.001).

In the last behavioral experiment, no antiallodynic effect was induced by the administration of the scavenger $p75^{NTR}$-Fc throughout the time interval examined (fig.17). Analysis of variance carried out in group 5 revealed no significant effect of treatment ($F_{1,16}$=0,46 p=.833) and time x treatment interaction ($F_{16,256}$=1,669 p=.06); only time had a significant effect ($F_{16,256}$=5,478 p<.001), probably due to the fluctuation visible on D3, D4, D14 and D17.

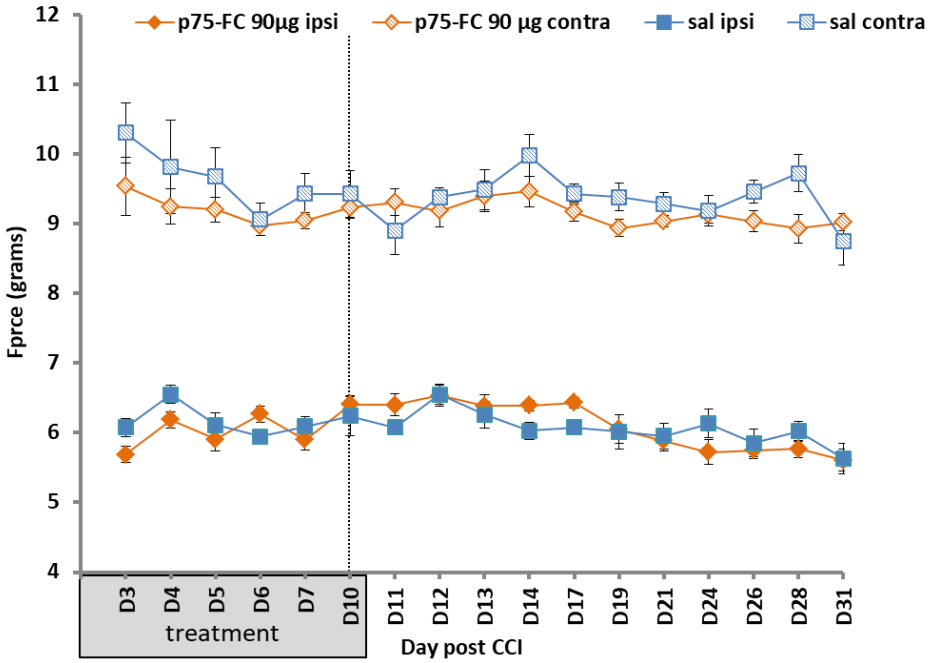

Figure17. Temporal trend of mechanical allodynia recorded in ipsilateral (ipsi) hindpaws. In orange is represented the group treated with 90µg/day of p75-Fc, in blue the controls injected with saline (sal). Open symbols refer to contralateral (contra) values. Values are expressed as means±SE.

Altogether, these data demonstrate that the blockade of the NGF pathway, through the sequestration of the protein itself or its receptor TrkA, is able to counteract neuropathic pain provoked by sciatic nerve ligature, in a dose-dependent manner, and that the antiallodynic effect obtained is strikingly long lasting.

4.2 Immunohistochemistry

4.2.1 Sciatic nerve.

4.2.1.1 CCI outcome

Among several events associated to the ligation procedure and to the consequent disruption of nerve fibers and myelin, there is the recruitment of Mast cells in the ligation site, as shown in figure 18.

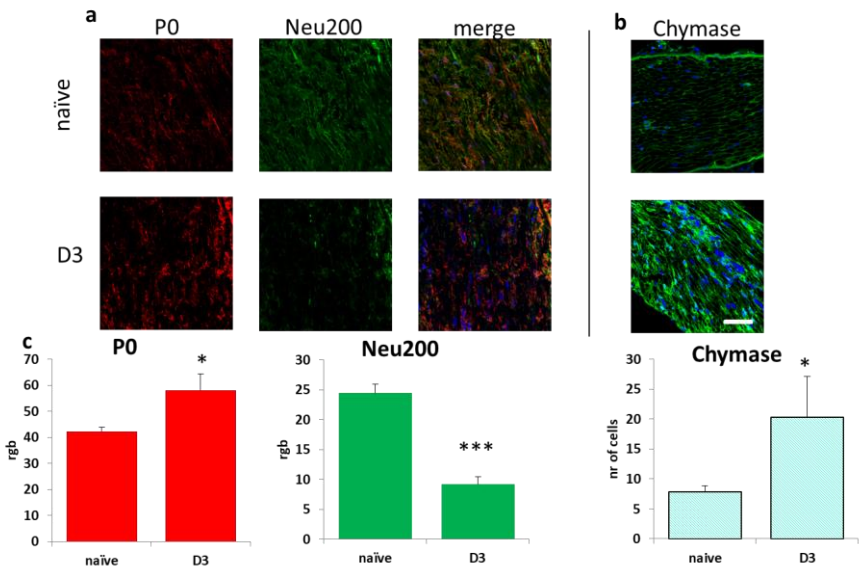

Figure18.a Representative examples of high magnification (63X) images of P0 (red), Neu200 (green) and merge (yellow) in sciatic nerve in naive mice and at D3 post CCI. Scale 50µm. **b** Chymase positive cells (turquoise). The **c** panel shows RGB quantification of P0 and Neu200, and Chymase positive cells count. Values are shown as mean±SE, *p<.05, ***p<.001

We have evaluated in naïve animals and neuropathic mice 3 days after CCI: i) the major structural protein of peripheral myelin, P0, which determines the thickness of myelin (Snipes GJ & Suter U, 1995); ii) the intermediate filament that constitutes a structural cytoskeletal element of axons, Neu200; and iii) the enzyme Chymase (Mast Cell Protease 1, also designated Mcp-1 or Mcpt1), protease found primarily in Mast cells, which allows to investigate the immune system activation and the level of inflammation. In D3 group P0 is present in a degenerated structure compared to naïve group, where the myelin is well distributed along fibers. The neurofilaments staining revealed a loss of the integrity of the fibers consequent to the ligature (fig.18a). The RGB analysis of florescence shows that P0 expression is significantly increased after CCI ($p<.05$), coherently with the formation of ovoids within the so called digestion chambers of Cajal (Wong KM et al., 2017), while Neu200 is significantly more expressed in naïve animals than in D3 post CCI ($p<.001$) (fig.17c), indicating axonal degeneration.. The statistical analysis of the Chymase positive cells revealed a significant increase of the number of Mast cells on D3, coherent with immune system recruitment necessary to promote tissue remodeling and nerve repair ($p<.05$) (fig.18c).

4.2.1.2 Effects of the treatments

To evaluate if the described damages were affected by treatments, we investigated P0 and Neu200 expression as well as Chymase and the expression of Schwann cells (S100β), at different time points post CCI, D11, D24 and D90.

The histological analysis permits the visualization of regenerating fibers (Neu200) in both treated groups. Even if no significant differences were found in the expressions of either P0 or Neu200 in comparison with saline (fig.19b and c), in MNAC13 and aD11 treated groups sciatic nerve appears to be better structured than in saline, where myelin is disorganized and neurofilaments are segmented (fig.19).

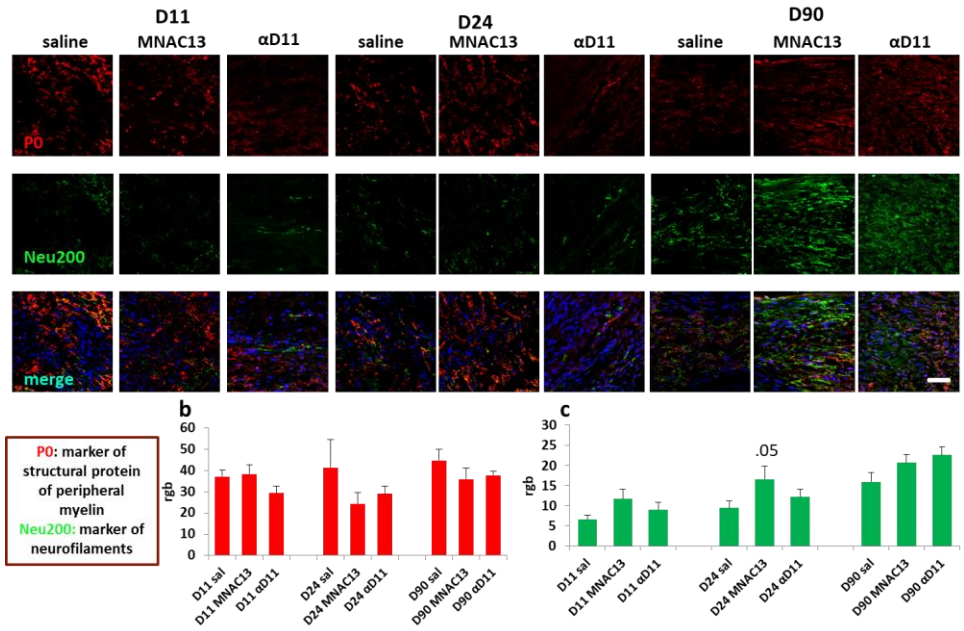

Figure 19. Representative examples of high magnification (63X) images of P0 (red), Neu200 (green) and merge (yellow) in sciatic nerve at D11, D24 and D90 post CCI. Scale 50µm. **b.** RGB quantification of P0. **c**. RGB quantification of Neu200. Values are shown as mean±SE

In figure 20 we can appreciate the expression of Schwann cells. Schwann cells respond to nerve damage strongly contributing to Wallerian degeneration (Chen P et al., 2015) that involves the dismantlement and clearance of injured axons and their myelin sheaths. The Schwann cells expression seems to be enhanced after MNAC13

administration at D11, suggesting a faster response to the injury; moreover, the structure of Schwann cells in all time points examined is better defined, while in control group is disorganized. Besides being important to study the immune response, Mast cells activation is strictly dependent on NGF pathway, and thus particularly suitable in our study. The immunostaining and the quantification of Mast cells revealed a strong reduction, likely due to the treatments present at each analyzed time point and lasting until D90 (fig.20).

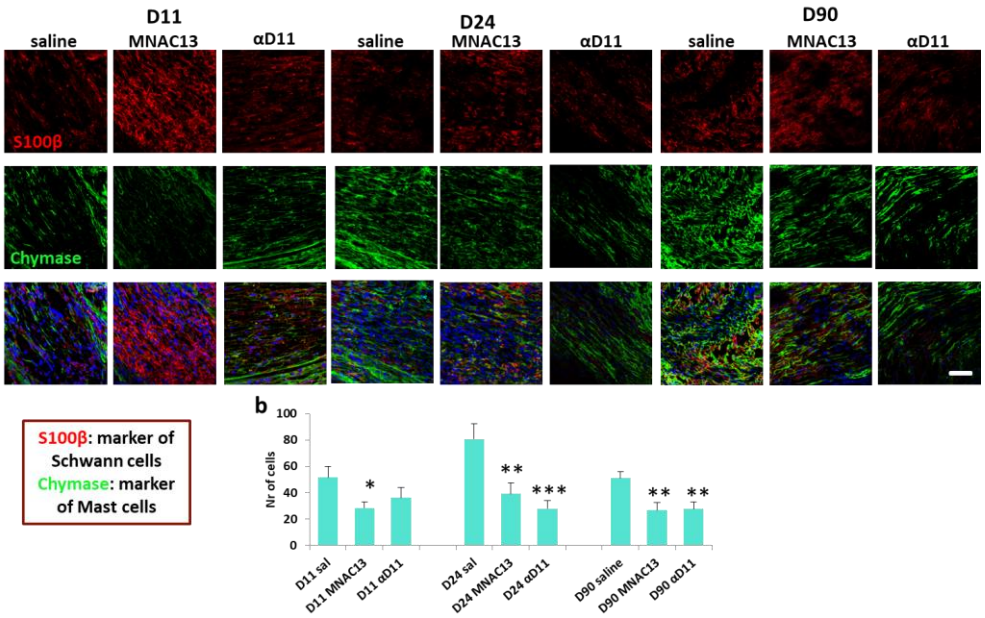

Figure 20. Representative examples of high magnification (63X) images of S100β (red), Chymase (green) in sciatic nerve at D11, D24 and D90 post CCI. Scale 50µm. **b** Chymase positive cells count. Values are shown as mean±SE, *p<.05, **p<.01, ***p<.001

4.2.2 Spinal cord

The staining of spinal cords sections gave us the possibility to investigate the central nervous system response to a peripheral insult, and to evaluate if the treatments with MNAC13 and αD11 are able to modify it. The analysis was performed targeting cells in laminae I-IV of Lumbar IV-V Dorsal Horns (DH), ipsilateral to the ligature. In particular we focused our attention on astrocytes (marked with GFAP) and microglia (marked with IBA1), to study their expression and morphology, and, through the co-localization with the phosphorylated MAPKinase p38 (p-p38), their activation. Analyses were performed on the same time points as the nerve.

4.2.2.1 CCI outcome

The analysis of the staining of SC 3 days after CCI revealed a fast and strong response to CCI in the central nervous system.

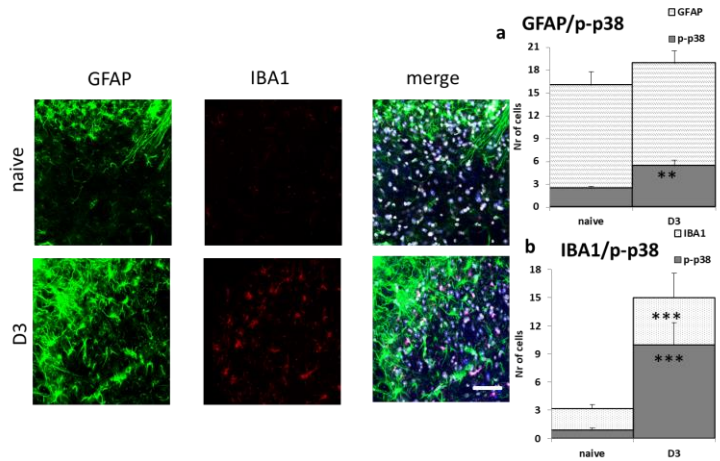

Figure 21. Representative images of high magnification (63x) ipsilateral dorsal horns in naïve and at D3 post CCI. Images show astrocytes (GFAP, green), microglia (IBA1, red) and colocalizations between them and p-p38 (marked in blue) and nuclei (marked in grey). Scale 50µm. **a.** GFAP positive cells count and co-localization with p-p38. **b.** IBA1 positive cells count and co-localization with p-p38. Values are shown as mean±SE, *p<.05, **p<.01, ***p<.001

We found an increase in the number of active astrocytes (naïve vs D3 p<.01), of microglia positive cells (naïve vs D3 p<.001) and active microglia (naïve vs D3 p<.001). In addition to the changes in the number, changes in the morphology of the cells are important too. Microglia are the first responder to the damage, reaching the peak of activation at D3 (Taves S et al., 2013), which is manifested through a switch from a ramified morphology to the ameboid.

4.2.2.2 Effect of the treatments

4.2.2.2.1 D11

The immunofluorescence performed at D11 reveals that astrocytes in control group are more hypertrophic than in treated animals, evidence that is confirmed also by RGB analysis of GFAP florescence (p<.001 sal vs both treatments). The statistical analysis performed on cells count revealed a significant reduction of astrocytes in the number (sal vs MNAC13 p<.001; sal vs αD11 p<.01) and in their activation (sal vs MNAC13 p<.001; sal vs αD11 p<.01) (fig.22).

The analysis of microglia revealed no difference in the morphology of the cells, being all of them in the ameboid active shape. Significant differences are present in the number (p<.01) and activation (p<.01), but only between controls and αD11 treated group.

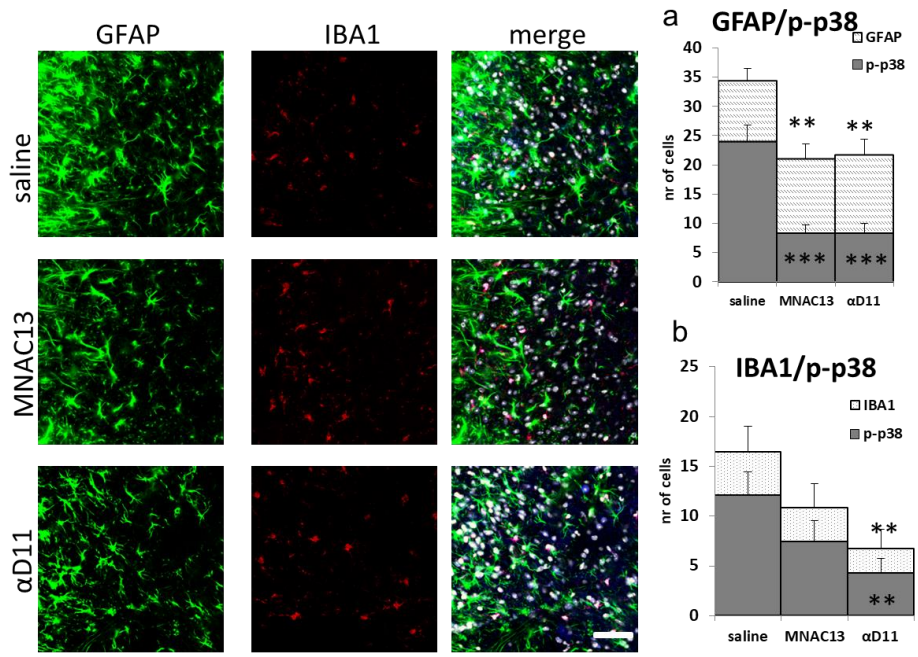

Figure 22. Representative images of high magnification (63x) ipsilateral dorsal horns at D11 post CCI. Images show astrocytes (GFAP, green), microglia (IBA1, red) and colocalizations between them and p-p38 (marked in blue) and nuclei (marked in grey). Scale 50µm. **a.** GFAP positive cells count and co-localization with p-p38. **b.** IBA1 positive cells count and co-localization with p-p38. Values are shown as mean±SE, *p<.05, **p<.01, ***p<.001

4.2.2.2.2 D24

The statistical analysis performed on D24 did not reveal any significant difference between treated and control groups in the parameters taken into account, as shown in figure 23. The anti-allodynic effect observed in this time window is therefore probably sustained by the modification at the periphery, already shown (fig.19, 20).

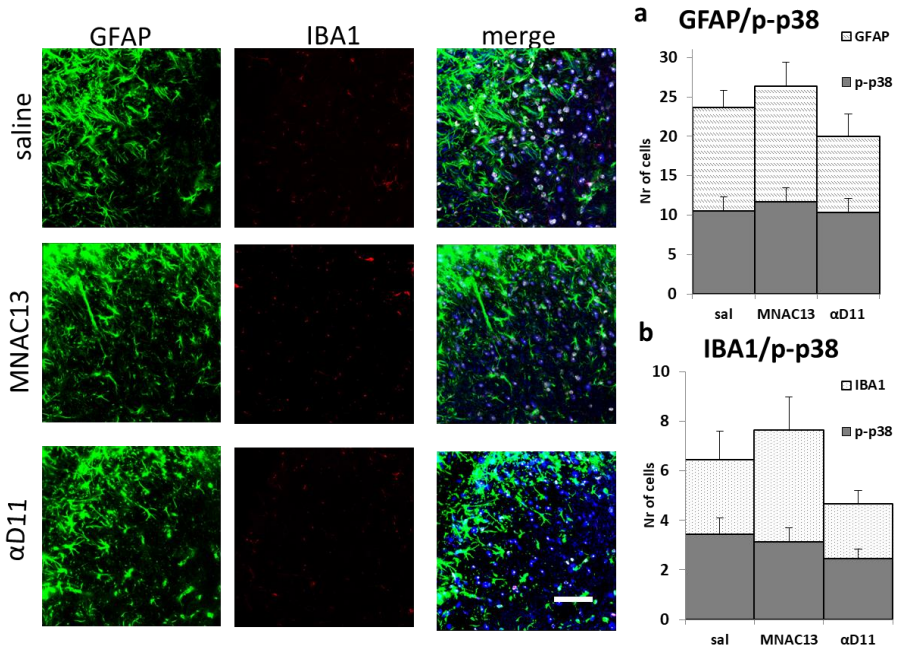

Figure 23. Representative images of high magnification (63x) ipsilateral dorsal horns at D24 post CCI. Images show astrocytes (GFAP, green), microglia (IBA1, red) and colocalizations between them and p-p38 (marked in blue) and nuclei (marked in grey). Scale 50μm. **a.** GFAP positive cells count and co-localization with p-p38. **b.** IBA1 positive cells count and co-localization with p-p38. Values are shown as mean±SE.

4.2.2.2.3 D90

In the last time point considered, D90, the analysis revealed that significant differences are still present in microglia (MNAC13 vs sal $p<.05$ number; $p<.05$ active cells) and in astrocytes (MNAC13 vs sal $p<.001$ number; MNAC13 vs sal $p<.05$ active cells) as concerns MNAC13; on the other hand significant differences for αD11 were observed in the activation of microglia (αD11 vs sal $p<.05$) and in the number astrocytes (αD11 vs sal $p<.01$) as shown by the colocalization

of GFAP and IBA1 with phosphorylated p38 (fig. 24). MNAC13 seems to have a stronger effect on glial cells than αD11.

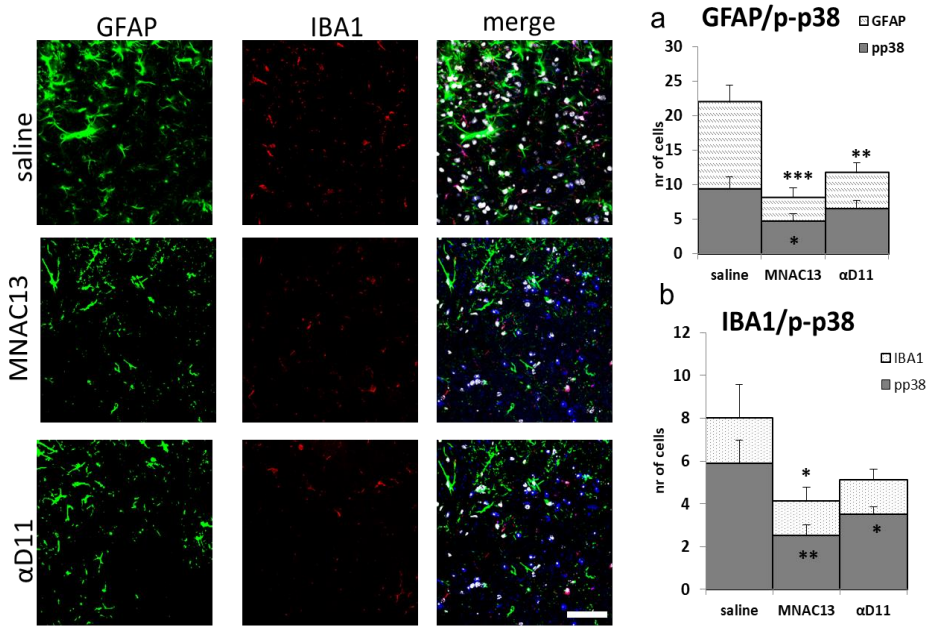

Figure 24. Representative images of high magnification (63x) ipsilateral dorsal horns at D90 post CCI. Images show astrocytes (GFAP, green), microglia (IBA1, red) and colocalizations between them and p-p38 (marked in blue) and nuclei (marked in grey). Scale 50µm. **a.** GFAP positive cells count and co-localization with p-p38. **b.** IBA1 positive cells count and co-localization with p-p38. Values are shown as mean±SE, *p<.05, **p<.01, ***p<.001

Figure 25 summarizes the immunohistochemical results, helping to compare changes during time among astrocyte and microglia positive and active cells in controls, MNAC13 and αD11 treated groups. After CCI the number and activation of astrocytes and microglia massively raise and increase until D11. These modifications indicate the presence of active gliosis, a set of changes that involve activation, proliferation and migration of astrocytes and microglia as an active response to the

lesion (Taves S et al., 2013). Treatments with the anti-TrkA and anti-NGF mAbs, strongly counteract this increase, as detectable at D11. At D24 control group shows a decrease in the number and activation of glial cells, resembling the treated groups and leading to the actual loss of difference among them. Differences between treated and controls are present again at D90. In saline group there is no decrease between D24 and D90, while treated groups, especially MNAC13, show further reduction of number and activation of astrocytes and microglia.

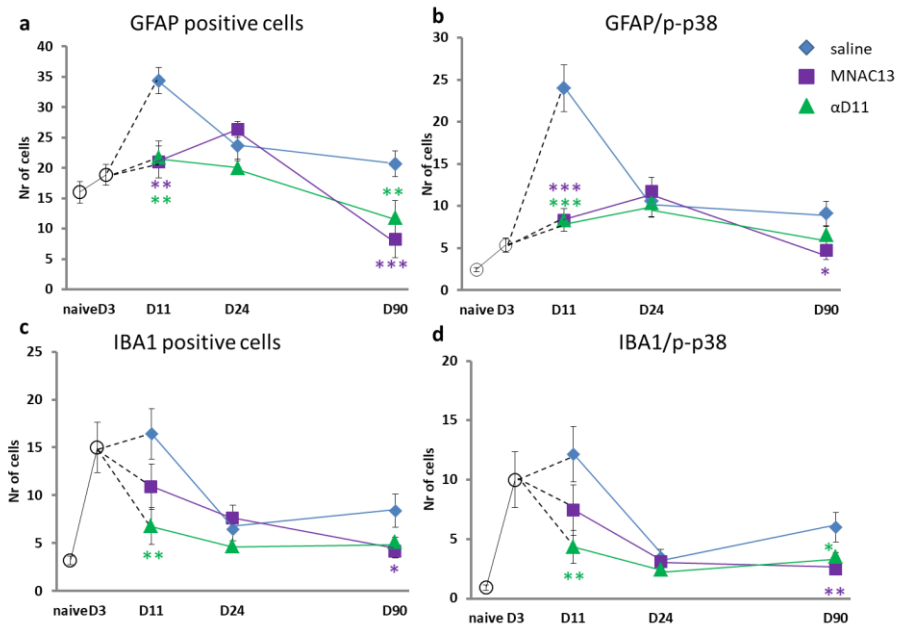

Figure25. Time trend of astrocyte number (**a**) and activation (**b**) and of microglia number (**c**) and activation (**d)** in spinal cord sections. In violet is represented the group treated with 100µg/day of MNAC13, in green the group treated with 100µg/day of αD11 and in blue the controls injected with saline. Open symbols refer to naïve and D3 values. Values are expressed as means±SE. *p<.05, **p<.01, ***p<.001; in black D3 vs naïve , in violet MNAC13 vs controls, in green αD11 vs controls.

4.3 ELISA

The values of sera obtained from CCI mice were all largely out of scale, also at very high dilutions. This issue was probably due to the high inflammation of the CCI mice, and to the consequent presence of IgG at high concentration. Many attempts were done to decrease this unspecific signal by using different additives and by diminishing the incubation times, however the obtained results were considered not reliable. The analysis is therefore referred to sera obtained from naïve mice treated with MNAC13,αD11 and saline.

4.3.1 MNAC13

ELISA assay showed that neat and MNAC13 spiked serum samples had good recovery and coefficients of variation, and consistent dilution values. The sera treated with saline were under the limit of detection. The measured values of sera of naïve mice treated with MNAC13 were consistent each other at different dilutions, and gave a good recovery if spiked with MNAC13.

The results demonstrate that anti-TrkA is present in serum at high concentrations and decreases slowly until it becomes very low or completely absent in some samples at D90.

Figure 26 reports the results of the MNAC13 PK: mean of three repeated measurements for each sample is shown. As evident, the MNAC13 concentration showed low variability, and a good recovery of the spiking.

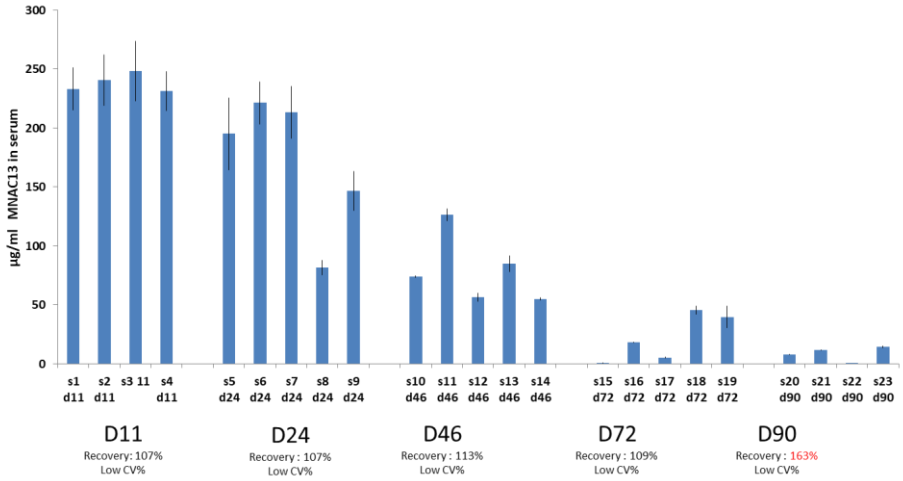

Figure26. Levels of MNAC13 (µg/ml) present in mice serum at different time points. Data show mean±SE for repeated measurements for each sample.

Figure 27 shows the average of the repeated measurements reported in figure 25. As evident, MNAC13 concentration decreases over time from D11 to D90.

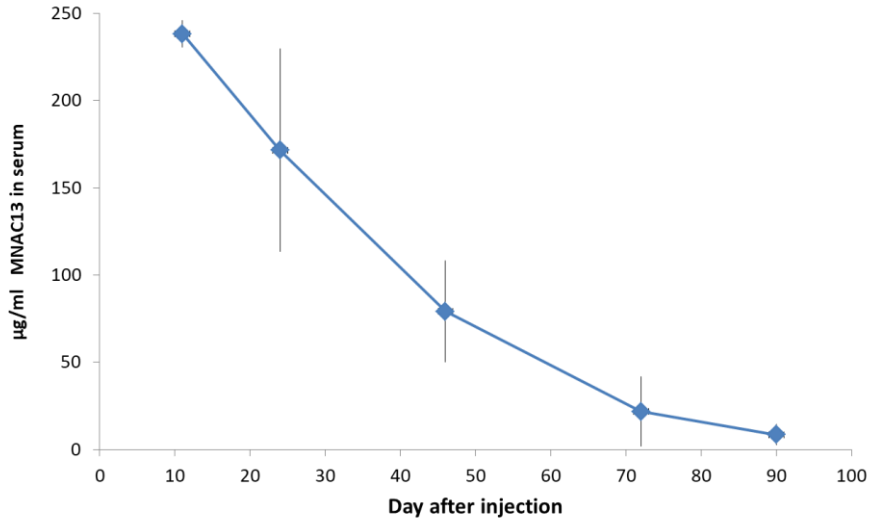

Figure27. Time trend of MNAC13 (µg/ml) present in mice serum at different time points. Data shown as total mean mean±SE.

4.3.2 αD11

Sera from saline-treated mice were under the limit of detection. All the checked samples exhibit low coefficients of variation for the duplicates. The measured values of sera from naïve animals treated with αD11 are characterized by a high variability. In the same time points, some αD11-treated sera were under the limit of the detection. These samples did not give a good recovery if spiked with αD11. Conversely, the measured values of other sera from αD11-treated naïve mice were consistent in each sample at different dilutions, and gave a good recovery if spiked with αD11. We can hypothesize that sera, where αD11 was not detected, contained free mouse NGF that competed with the coated NGF in capturing αD11.

The Figure 28 reports the results of the αD11 PK of repeated measurements for each sample.

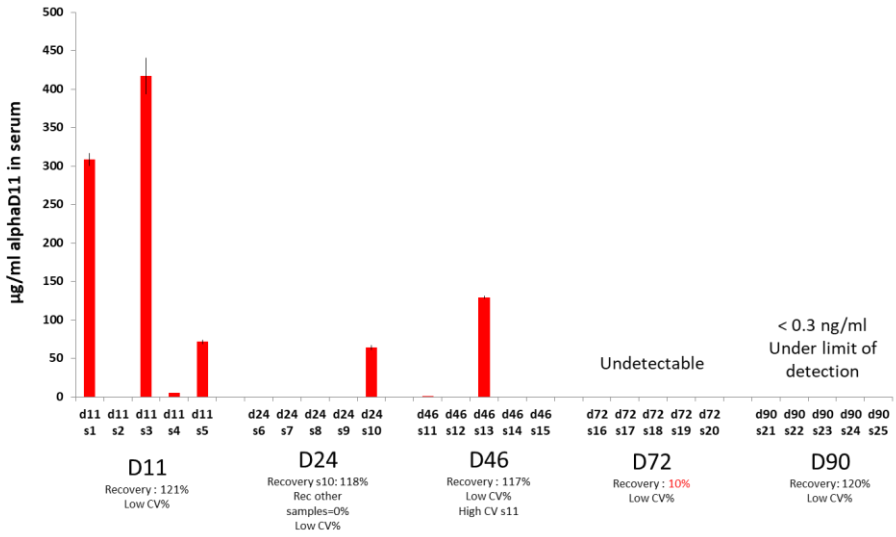

Figure28. Levels of αD11 present in mice serum at different time points. Data show mean±SE for repeated measurements for each sample

Despite the observed variability, αD11 concentration decreased in the time scale. At D72 the αD11 concentration was undetectable, because of the poor recovery. We can hypothesize that the αD11 concentration is so low that the antibody is completely captured by the free NGF. Conversely, at D90 αD11 concentration being under the limit of detection of the assay, there is indeed a good recovery of the spiking.

4.4 Immunoprecipitation

We incubated the membrane with ECL advance (GE Healtcare Life Science, Amersham ECL Select) and in order to optimize the results we used several exposures times, the first exposure times were for 4 and 8 minutes.

4.4.1 MNAC13

Since there was no difference between 4 and 8 minutes among the groups, the image shown is relative to the 4 minutes incubation.

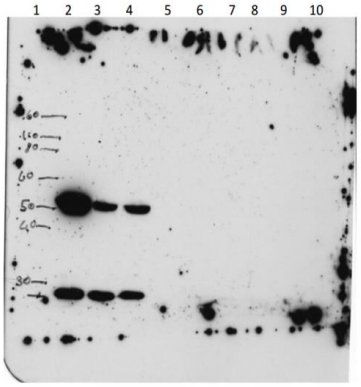

Figure 29. IP and WB of brain tissues from naïve and CCI mice. Samples order: 1. molecular weight marker; 2. MNAC13 mAb; 3. naive saline + biotinylated MNAC13; 4. CCI saline + biotinylated MNAC13; 5. naive saline; 6. CCI saline; 7. naive 1 MNAC13; 8. naive 2 MNAC13; 9. CCI 1 MNAC13; 10. CCI2 MNAC13. 4 minutes ECL exposure.

The results clearly show that only positive controls are visible, thus MNAC13 is not present in brain tissue of mice and we can conclude that it does not pass through the Blood Brain Barrier.

4.4.2 αD11

In this experiment, since the background was strong (fig.30a) we further reduced the exposure and exposed for 30 seconds (fig.30b).

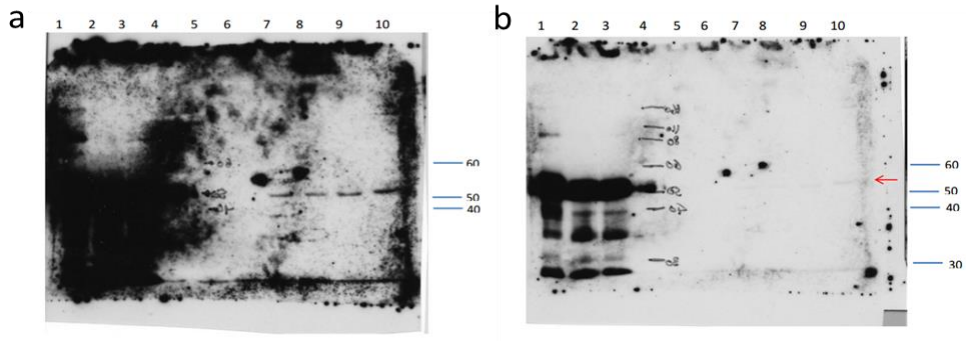

Figure 30. IP and WB of brain tissues from naïve and CCI mice . Samples order: 1. aD11 mAb ; 2. naive saline + biotinylated αD11; 3. CCI saline + biotinylated αD11; 4. molecular weight marker; 5. naive saline; 6. CCI saline; 7. naive 1 αD11; 8. naive 2 αD11; 9. CCI 1 αD11; 10. CCI2 αD11. a 4 minutes and b 30 seconds ECL exposure

Besides being the controls very strong, bands at 50 KDa, height of the heavy chain of the MAb, are clearly visible in naïve and CCI sample, but not in controls. The interpretation of the results is clear even if there is a strong background. The 30' exposure reduces the strength of controls but samples bands still remain visible. It is thus demonstrated that anti-NGF is able to cross Blood Brain Barrier.

Chapter V: Discussion

After CCI C57BL/6J mice develop sustained and long lasting mechanical allodynia. This behavioral outcome is sustained by relevant changes in the sciatic nerve: i) nerve fibers are damaged, together with the myelin sheaths and the Schwann cells structure; ii) the immune system rapidly responds to the damage, in particular Mast cells that are activated and recruited in the lesion site. In L4-L5 spinal cord dorsal horns glial cells respond to the lesion too. Microglia and astrocytes respond to the peripheral damage with an active process known as active gliosis, consisting in changes in morphology, proliferation, migration and upregulation of inflammatory markers.

With this project we demonstrated the efficacy of the two antibodies anti-TrkA MNAC13 and anti-NGF αD11 to counteract pain features in our model of neuropathic pain. We indeed provided evidence that antibodies have a strikingly long lasting antiallodynic effects, and that these effects are well-supported by morphological and functional changes in central and peripheral nervous system.

As far as MNAC13 is concerned, behavioral evaluation demonstrated that intraperitoneal repeated administrations (8 days) were able to induce significant increase in the mechanical threshold of CCI mice. The initial dose, 70µg/mouse/i.p., had an effect on pain perception, reducing allodynia, which, however, only lasted until D21 post-surgery (fig.12). The second dose, increased at 100µg/mouse/i.p, was able not only to induce analgesia, but also to maintain its effect until D130 (fig.14 & 16).

To better understand the behavioral outcome, we compared tissues from treated mice with saline injected group, highlighting important differences in inflammatory and nerve regeneration processes. In treated group

neurofilaments, myelin and Schwann cells were less damaged than in controls, and nerve regeneration appeared in a more advanced state. These structural differences were driven by a strong and fast reduction in Mast cells presence at the lesion site (fig. 18,19). The blockade of TrkA receptor on these cells prevented their activation and therefore the recruitment of other immune cells, reducing inflammation and promoting structural recovery of the tissue. Consequences of the effects of MNAC13 in the periphery were also detectable in central nervous system.

In the first time point analyzed, D11, we found a significant reduction in number and activation of astrocytes, but not in microglia (fig.21). The effects on astrocytes might be attributable to the reduction of peripheral inflammation. The reduction of inflammatory activity in the nerve prevents the activation of astrocytes in the spinal cord, which drives the analgesic effects. The absence of statistically significant differences in microglia number and activation, even if a tendency towards reduction was present, might be due to the evidence that astrocytes become active at a slightly later time point than microglia. Microglia responds within 24 h following nerve injury and microgliosis becomes well established by day 3 post-injury (Richner M et al., 2014). We confirmed this evidence in our experiment with a strong activation and proliferation observed 3 days after the peripheral lesion (fig.20). Their activity has a peak around a week after the insult, and then spontaneously decreases. In our analysis we focused on D11 after surgery, since we wanted to have a picture of changes right after the end of the treatment, which lasted until D10. With the choice of this time point, we may have lost the time window to appreciate MNAC13 effects on microglia.

The spontaneous reduction over time of glial cells number and activation led to the loss of a statistically significant difference between groups in the

second time point, D24. On the other hand, while in MNAC13 treated group no differences are present either in glial cells number or in the activation between D11 and D24, in control group a robust decrease is evident (fig.24). In the last time point, D90, while in control group there are no changes in glial parameters compared to the previous time point, we found a further decrease in all the analyzed markers in MNAC13 group (fig.23).

Given these results we can speculate that the long lasting effect of the anti-TrkA mAb we found in the behavioral assay is ascribable to the central reduction of gliosis. While in the first phase glial reduction might be driven by the precocious reduction of inflammation, which triggers the analgesic effect, the absence of differences between D11 and D24 might be due to epigenetic changes in spinal cord. Acetylation and methylation are processes that require longer time to take place; it is thus possible that these modifications start after the acute effect of the mAb, leading to the long lasting antihyperalgesic effect. Indeed, further significant reduction in glial number and activation is present at D90. The pharmacokinetics assay supports this hypothesis. MNAC13 had a long time clearance, that was consistent in all samples. Even if the antibody remained for two months in the blood stream, at D90 it was substantially absent (fig.25-26), confirming that the results we found were not imputable to the compound in circulation. Also, MNAC13 was not able to cross the Blood Brain Barrier, demonstrating that the central changes we found were not consequence of a direct action of the antibody itself.

Behavioral evaluation of αD11 treated mice demonstrated that intraperitoneal repeated administration (8 days) was able to induce significant increase in the mechanical threshold of CCI mice. As reported for anti-TrkA, the initial dose administered, 70µg/mouse/i.p., reduced

allodynia, but the effect disappeared after a month (fig.13). The second dose, increased at 100µg/mouse/i.p, in this case too, induced analgesia lasting until D90 post-surgery (fig.15).

The histological analysis performed was the same carried on for MNAC13.

Compared to saline, αD11 treated group had a better regenerating nerve, myelin and Schwann cells structure, and a strong reduction in Mast cells number and activation. Compared with anti-TrkA, anti-NGF effects result to be delayed in time. The reduction of Mast cells number become statistically significant only starting from D24, while at D11only a tendency is present. Moreover, the morphology of the myelin and of the Schwann cells seems to ameliorate faster in MNAC13 group than αD11 (fig.18,19). These differences might be due to the different way of action of the mAbs. MNAC13 acts on the receptor, factually preventing NGF to bind and display its action. αD11 acts on the protein, it is therefore more difficult to prevent the binding since it takes longer to capture the circulating molecules.

Regarding spinal cord, a strong reduction was found in astrocytes and microglia number and activation in the first time point, differently from MNAC13 were microglia was not significantly reduced (fig.21). These data seem to contradict our hypothesis of two different time courses for astrocytes and microglia. An explanation could be found in the results obtained in the immunoprecipitation. αD11 is in fact able to cross the Blood Brain Barrier, and can therefore prevent NGF/TrkA binding directly acting on glial cells, reducing their number and activation. The outcome is that microglia continues to be downregulated compared to MNAC13, which instead displays its action indirectly.

At D24 and D90 the results were consistent with MNAC13 ones, even if the late effect (D90) of αD11 was present only in the number of astrocytes and the activation of microglia (fig.23). The pharmacokinetics of anti-NGF, despite being more variable between samples, showed a clearance faster than that observed in anti-TrkA; anyhow, as shown, both mAbs were absent in serum at D90 (fig.27).

Since αD11 is no longer present in the blood stream, the long lasting effect might be due to initial peripheral action of the antibody that reduces inflammation and degeneration, and to subsequent epigenetic changes, as seen for MNAC13. However, the central effect of αD11 makes it more difficult to give a final interpretation of the results. It might also be possible that the direct effect on CNS at D11 influences itself the late glial activation, potentiating peripheral effects and helping maintaining analgesia.

As mentioned above, the presence of antiallodynic effects after the clearance of the mAbs rise the hypothesis that MNAC13 and αD11 might trigger epigenetic mechanisms that might support analgesia and the changes in peripheral and central nervous system.

Epigenetic changes are present in neuropathic pain and are fundamental to sustain and maintain sensitization phenomena (Wang J et al., 2017; Shao C et al., 2017). Anti-TrkA and anti-NGF might counteract these changes or *per se* induce epigenetic modification, promoting analgesia and nerve regeneration.

The EBRI Genomics facility, also involved in the "Paincage" European project, carried on a wide gene expression analysis to identify genes modulated in neuropathic pain before and after treatments.

Even if differences between the mAbs were found, due to the different Blood-Brain Barrier permeability, the direction of the effects is similar,

since both tend to downregulate gene expression, which instead is upregulated by CCI. The main similarities are found in genes that regulate glutamatergic and GABAergic neurotransmission, whose balance is crucial for pain perception (Yusuf MS & Kerr BJ; 2016). In fact, after chronic constriction of the sciatic nerve, higher levels of Glu and lower levels of GABA compared to control animals were observed; moreover, increased levels of Glu or decreased endogenous levels of GABA in naïve rats led to thermal hyperalgesia and mechanical allodynia (Watson CJ; 2016). MNAC13 and αD11 modify receptor sub-units of both amino acids in an opposite direction compared to CCI effect.

The treatments with the anti-TrkA and anti-NGF are therefore able to counteract gene expression alterations driven by CCI, demonstrating that the modification we found in behavior, morphology, inflammation and cellular activation markers are supported by deep epigenetic changes.

Moreover, the individuation of modifications of specific genes will help to further characterize molecular mechanisms of action of the mAbs. In addition, they will contribute to the identification of new biomarkers, allowing better patient stratification, and possibly become themselves focus of future treatments for neuropathic pain.

Concerning $p75^{NTR}$-Fc, while it results to be effective in OA models, we did not find any difference between treated and control groups. A possible explanation for the lack of analgesic effects relies in the model itself. In CCI high levels of NGF are released in the lesion site by nerve endings, resident Schwann cells and Mast cells; in OA model most of the NGF is produced by fibroblasts and Mast cells (Manni L et al., 2003), and by chondrocytes after increase of the mechanical load of the cartilage (Pecchi E et al., 2014). It is possible that NGF levels in CCI are so high that the amount that bind $p75^{NTR}$-Fc is not enough to reduce hyperalgesia. In OA

the scavenger might be effective because NGF levels may rise in a secondary phase, after the establishment of the cartilage damage.

CONCLUSIONS

Neuropathic pain is as a complex and heterogeneous condition. It is very common among general population; in western countries its prevalence is estimated to be between 6.9% and 10%. In clinical practice is a deeply debilitating problem, in fact neuropathic pain is often refractory to common analgesics and treatment, and patients suffer from more pain severity, greater costs, and relatively impaired quality of life. Reducing its impact and improving the quality of life of millions of patients is therefore a compelling challenge.

In this sense our study perfectly responds to the need of new treatments arisen in the past years.

We carried on a comparison between the therapeutic effectiveness of new generation NGF-targeting drugs as neuropathic pain treatments.

We can conclude that after MNAC13 and αD11 treatments:

- hyperalgesia is efficaciously counteracted;
- the analgesic effects are maintained long lasting, overcoming the presence of the compounds in the bloodstream;
- the effects are not dependent on the presence of the mAbs;
- the effects are correlated withchanges in peripheral inflammatory response and nerve structure;
- morphological and immune system changes in the periphery correlate with changes in CNS,where glial activation is reduced;
-reduction of glial activation might be due to epigenetic changes;
- reduced glial activation in CNS supports the long lasting maintenance of analgesic effect.

While for αD11 more details have to be clarified, such as the amount of the antibody that reaches CNS and the time needed for its clearance, as well as the possible impact in safety, MNAC13 seems to be extremely promising for human trials.

The long lasting analgesic effects of this compound might reduce the daily dose intake, increasing patients' compliance to the treatment. We hope that the results of this study will provide information for the development of new and more effective analgesic drugs. Better compliance and better analgesic effects will reflect on the social side of chronic pain issue, strongly increasing quality of life of patients suffering from neuropathic pain, with an additional great reduction of social costs due to actual inadequate pain treatment.

BIBLOGRAPHY

Aalto K, Korhonen L, Lahdenne P, Pelkonen P, Lindholm, D. *Nerve growth factor in serum of children with systemic lupus erythematosus is correlated with disease activity*. Cytokine. 2002 Nov 7;20(3):136-9.

Aloe L, Tuveri M.A, Carcassi U, Levi-Montalcini R. *Nerve growth factor in the synovial fluid of patients with chronic arthritis.* Arthritis Rheum. 1992 Mar;35(3):351-5.

Barthel C, Yeremenko N, Jacobs R, Schmidt RE, Bernateck M, Zeidler H, Tak PP, Baeten D, Rihl M. *Nerve growth factor and receptor expression in rheumatoid arthritis and spondyloarthritis.* Arthritis Res Ther. 2009;11(3):R82. doi: 10.1186/ar2716. Epub 2009 Jun 2.

Beniczky S, Tajti J, Tímea Varga E, Vécsei L. *Evidence-based pharmacological treatment of neuropathic pain syndromes*. J Neural Transm (Vienna). 2005 Jun;112(6):735-49.

Bennett GJ, Xie YK. *A peripheral mononeuropathy in rat that produces disorders of pain sensation like those seen in man*. Pain. 1988 Apr;33(1):87-107.

Bibel M, Hoppe E, Barde YA. *Biochemical and functional interactions between the neurotrophin receptors trk and p75NTR*. EMBO 1999. J. 18:616–22

Bonakdar RA. *Integrative Pain Management Medical Clinics of North America* Volume 101, Issue 5, September 2017, Pages 987-1004

Bracci-Laudiero L, Aloe L, Levi-Montalcini R, Buttinelli C, Schilter D, Gillessen S, Otten U. *Multiple sclerosis patients express increased levels of B-nerve growth factor in cerebrospinal fluid.* Neurosci. Lett. 1992, 147, 9–12

Bracci-Laudiero L, Aloe L, Levi-Montalcini R, Galeazzi M, Schilter D, Scully JL, Otten U. *Increased levels of NGF in sera of systemic lupus erythematosus patients.* Neuro. Report 1992, 4, 563–565.

Bracci-Laudiero L, Lundeberg T, Stenfors C, Theodorsson E, Tirassa P, Aloe L. *Modification of lymphoid and brain nerve growth factor levels in systemic lupus erythematosus mice.* Neurosci. Lett. 1996, 204, 13–16

Capsoni S, Covaceuszach S, Marinelli S, Ceci M, Bernardo A, Minghetti L, Ugolini G, Pavone F, Cattaneo A. *Taking pain out of NGF: a "painless" NGF mutant, linked to hereditary sensory autonomic neuropathy type V, with full neurotrophic activity*. PLoS One. 2011 Feb 28;6(2):e17321. doi: 10.1371/journal.pone.0017321.

Cattaneo A, Capsoni S, Margotti E, Righi M, Kontsekova E, Pavlik P, Filipcik P, Novak M. *Functional blockade of tyrosine kinase A in the rat basal forebrain by a novel antagonistic anti-receptor monoclonal antibody.* J Neurosci. 1999 Nov 15;19(22):9687-97.

Cattaneo A, Rapposelli B, Calissano P. *Three distinct types of monoclonal antibodies after long-term immunization of rats with mouse nerve growth factor.* J Neurochem. 1988 Apr;50(4):1003-10.

Cattin AL, Lloyd AC. *The multicellular complexity of peripheral nerve regeneration.* Curr Opin Neurobiol. 2016 Aug;39:38-46. doi: 10.1016/j.conb.2016.04.005. Epub 2016 Apr 26

Chang DS, Hsu E, Hottinger DG, Cohen SP. *Anti-nerve growth factor in pain management: current evidence.* J Pain Res. 2016 Jun 8;9:373-83. doi: 10.2147/JPR.S89061. eCollection 2016.

Chen P, Piao X, Bonaldo P. *Role of macrophages in Wallerian degeneration and axonal regeneration after peripheral nerve injury.* Acta Neuropathol. 2015 Nov;130(5):605-18. doi: 10.1007/s00401-015-1482-4. Epub 2015 Sep 29.

Cobianchi S, Marinelli S, Florenzano F, Pavone F, Luvisetto S. *Short- but not long-lasting treadmill running reduces allodynia and improves functional recovery after peripheral nerve injury.* Neuroscience. 2010 Jun 16;168(1):273-87. doi: 10.1016/j.neuroscience.2010.03.035. Epub 2010 Mar 25.

Covaceuszach S, Cassetta A, Cattaneo A, Lamba D. *Purification, crystallization, X-ray diffraction analysis and phasing of a Fab fragment of monoclonal neuroantibody alphaD11 against nerve growth factor.* Acta Crystallogr D Biol Crystallogr. 2004 Jul;60(Pt 7):1323-7. Epub 2004 Jun 22.

Covaceuszach S, Cattaneo A, Lamba D. *Neutralization of NGF-TrkA receptor interaction by the novel antagonistic anti-TrkA monoclonal antibody MNAC13: a structural insight.* Proteins. 2005 Feb 15;58(3):717-27.

Covaceuszach S, Marinelli S, Krastanova I, Ugolini G, Pavone F, Lamba D, Cattaneo A. *Single cycle structure-based humanization of an anti-nerve growth factor therapeutic antibody.* PLoS One. 2012;7(3):e32212. doi: 10.1371/journal.pone.0032212. Epub 2012 Mar 5.

Denk F, Bennett DL, McMahon SB. *Nerve Growth Factor and Pain Mechanisms.* Annu Rev Neurosci. 2017 Jul 25;40:307-325. doi: 10.1146/annurev-neuro-072116-031121. Epub 2017 Apr 24.

Dyck PJ, Peroutka S, Rask C, Burton E, Baker MK, Lehman KA, Gillen DA, Hokanson JL, O'Brien PC. *Intradermal recombinant human nerve growth factor induces pressure allodynia and lowered heat-pain threshold in humans.* Neurology. 1997 Feb;48(2):501-5.

Fukui Y, Ohtori S, Yamashita M, Yamauchi K, Inoue G, Suzuki M, Orita S, Eguchi Y, Ochiai N, Kishida S, Takaso M, Wakai K, Hayashi Y, Aoki Y, Takahashi K. *Low affinity NGF receptor (p75 neurotrophin receptor) inhibitory antibody reduces pain behavior and CGRP expression in DRG in the mouse sciatic nerve crush model.* J Orthop Res. 2010 Mar;28(3):279-83. doi: 10.1002/jor.20986.

Gaskin DJ, Richard P. *The economic costs of pain in the United States.* J Pain. 2012 Aug;13(8):715-24. doi: 10.1016/j.jpain.2012.03.009. Epub 2012 May 16.

Gozes I, Milner RJ, Liu FT, Johnson E, Battenberg EL, Katz DH, Bloom FE. *Monoclonal antibodies against vasoactive intestinal polypeptide: studies of structure and related antigens.* J Neurochem. 1983 Aug;41(2):549-55.

Gracely RH, Lynch SA, Bennett GJ. *Painful neuropathy: altered central processing maintained dynamically by peripheral input.* Pain. 1992 Nov;51(2):175-94.

Grichnik KP, Ferrante FM. *The difference between acute and chronic pain.* Mt Sinai J Med. 1991 May;58(3):217-20.

Hempstead BL, Martin-Zanca D, Kaplan DR, Parada LF, Chao MV. *High-affinity NGF binding requires coexpression of thetrkproto-oncogene and the low-affinity NGF receptor*. Nature 1991 350:678–83

Hefti FF, Rosenthal A, Walicke PA, Wyatt S, Vergara G, Shelton DL, Davies AM. *Novel class of pain drugs based on antagonism of NGF*. Trends Pharmacol Sci. 2006 Feb;27(2):85-91. Epub 2005 Dec 27.

Hirose M, Kuroda Y, Murata E. *NGF/TrkA Signaling as a Therapeutic Target for Pain*. Pain Pract. 2016 Feb;16(2):175-82. doi: 10.1111/papr.12342. Epub 2015 Aug 27.

Hirose M, Takatori M, Kuroda Y, Abe M, Murata E, Isada T, Ueda K, Shigemi K, Shibazaki M, Shimizu F, Hirata M, Fukazawa K, Sakaguchi M, Kageyama K, Tanaka Y. *Effect of synthetic cell-penetrating peptides on TrkA activity in PC12 cells.* J Pharmacol Sci. 2008 Jan;106(1):107-13. Epub 2008 Jan 11.

Huang EJ, Reichardt LF. *Trk receptors: roles in neuronal signal transduction.* Annu Rev Biochem. 2003;72:609-42. Epub 2003 Mar 27.

Inman CF, Rees LE, Barker E, Haverson K, Stokes CR, Bailey M. *Validation of computer-assisted, pixel-based analysis of multiple-colour immunofluorescence histology.* J Immunol Methods. 2005 Jul;302(1-2):156-67.

Jaggi AS, Jain V, Singh N. *Animal models of neuropathic pain.* Fundam Clin Pharmacol. 2011 Feb;25(1):1-28. doi: 10.1111/j.1472-8206.2009.00801.x.

Ji RR, Berta T, Nedergaard M. *Glia and pain: is chronic pain a gliopathy?* Pain. 2013 Dec;154 Suppl 1:S10-28. doi: 10.1016/j.pain.2013.06.022. Epub 2013 Jun 20.

Ji RR, Suter MR. *p38 MAPK, microglial signaling, and neuropathic pain.* Mol Pain. 2007 Nov 1;3:33.

Khodorova A, Nicol GD, Strichartz G *The TrkA receptor mediates experimental thermal hyperalgesia produced by nerve growth*

factor: Modulation by the p75 neurotrophin receptor. Neuroscience Volume 340, 6 January 2017, Pages 384-397.

Khodorova A, Nicol GD, Strichartz G. *The p75NTR signaling cascade mediates mechanical hyperalgesia induced by nerve growth factor injected into the rat hind paw.* Neuroscience. 2013 Dec 19;254:312-23. doi: 10.1016/j.neuroscience.2013.09.046. Epub 2013 Oct 1.

Korsching S, Auburger G, Heumann R, Scott J, Thoenen H. *Levels of nerve growth factor and its mRNA in the central nervous system of the rat correlate with cholinergic innervation.* EMBO J. 1985 Jun;4(6):1389-93.

Lamb K, Kang YM, Gebhart GF, Bielefeldt K. *Nerve growth factor and gastric hyperalgesia in the rat.* Neurogastroenterol Motil. 2003 Aug;15(4):355-61.

Large TH, Bodary SC, Clegg DO, Weskamp G, Otten U, Reichardt LF. *Nerve growth factor gene expression in the developing rat brain.* Science. 1986 Oct 17;234(4774):352-5.

Lewin GR, Rueff A, Mendell LM. *Peripheral and central mechanisms of NGF-induced hyperalgesia.* Eur J Neurosci. 1994 Dec 1;6(12):1903-12.

Lindholm D, Heumann R, Meyer M, Thoenen H. *Interleukin-1 regulates synthesis of nerve growth factor in non-neuronal cells of rat sciatic nerve.* Nature. 1987 Dec 17-23;330(6149):658-9.

Liu M, Wood JN. *The roles of sodium channels in nociception: implications for mechanisms of neuropathic pain*. Pain Med 2011;12(Suppl 3):S93–9.

Luvisetto S, Marinelli S, Cobianchi S, Pavone F. *Anti-allodynic efficacy of botulinum neurotoxin A in a model of neuropathic pain.* Neuroscience. 2007 Mar 2;145(1):1-4. Epub 2007 Jan 9.

Mamet J, Lazdunski M, Voilley N. *How nerve growth factor drives physiological and inflammatory expressions of acid-sensing ion channel 3 in sensory neurons.* J. Biol. Chem. 2003, 278, 48907–48913.

Manni L, Aloe L. *Role of IL-1 and TNF-α in the regulation of NGF in experimentally induced arthritis in mice.* Rheumatol Int. 1998;18(3):97-102.

Manni L, Lundeberg T, Fiorito S, Bonini S, Vigneti E, Aloe L. *Nerve growth factor release by human synovial fibroblasts prior to and following exposure to tumor necrosis factor-alpha, interleukin-1 beta and cholecystokinin-8: the possible role of NGF in the inflammatory response.* Clin Exp Rheumatol. 2003 Sep-Oct;21(5):617-24.

Marinelli S, Luvisetto S, Cobianchi S, Makuch W, Obara I, Mezzaroma E, Caruso M, Straface E, Przewlocka B, Pavone F. *Botulinum neurotoxin type A counteracts neuropathic pain and facilitates functional recovery after peripheral nerve injury in animal*

models. Neuroscience. 2010 Nov 24;171(1):316-28. doi: 10.1016/j.neuroscience.2010.08.067. Epub 2010 Sep 6.

Meacham K, Shepherd A, Mohapatra DP, Haroutounian S. *Neuropathic Pain: Central vs. Peripheral Mechanisms.* Curr Pain Headache Rep. 2017 Jun;21(6):28. doi: 10.1007/s11916-017-0629-5.

Minnone G, De Benedetti F, Bracci-Laudiero L. *NGF and Its Receptors in the Regulation of Inflammatory Response.* Int J Mol Sci. 2017 May 11;18(5). pii: E1028. doi: 10.3390/ijms18051028.

Nencini S, Ringuet M, Kim DH, Chen YJ, Greenhill C1, Ivanusic JJ. *Mechanisms of nerve growth factor signaling in bone nociceptors and in an animal model of inflammatory bone pain*. Mol Pain. 2017 Jan;13:1744806917697011. doi: 10.1177/1744806917697011.

Norman BH, McDermott JS. *Targeting the Nerve Growth Factor (NGF) Pathway in Drug Discovery. Potential Applications to New Therapies for Chronic Pain.* J Med Chem. 2017 Jan 12;60(1):66-88. doi: 10.1021/acs.jmedchem.6b00964. Epub 2016 Oct 25.

Pecchi E, Priam S, Gosset M, Pigenet A, Sudre L, Laiguillon MC, Berenbaum F, Houard X. *Induction of nerve growth factor expression and release by mechanical and inflammatory stimuli in chondrocytes: possible involvement in osteoarthritis pain.* Arthritis Res Ther. 2014 Jan 20;16(1):R16. doi: 10.1186/ar4443.

Pertens E, Urschel-Gysbers BA, Holmes M, Pal R, Foerster A, Kril Y, Diamond J. *Intraspinal and behavioral consequences of nerve growth factor-induced nociceptive sprouting and nerve growth factor-induced hyperalgesia compared in adult rats.* J Comp Neurol. 1999 Jul 19;410(1):73-89.

Rapp AE, Kroner J, Baur S, Schmid F, Walmsley A, Mottl H, Ignatius A. *Analgesia via blockade of NGF/TrkA signaling does not influence fracture healing in mice.* J Orthop Res. 2015 Aug;33(8):1235-41. doi: 10.1002/jor.22892. Epub 2015 May 7.

Richner M, Ulrichsen M, Elmegaard SL, Dieu R, Pallesen LT, Vaegter CB. *Peripheral nerve injury modulates neurotrophin signaling in the peripheral and central nervous system.* Mol Neurobiol. 2014 Dec;50(3):945-70. doi: 10.1007/s12035-014-8706-9. Epub 2014 Apr 22.

Sevcik MA, Ghilardi JR, Peters CM, Lindsay TH, Halvorson KG, Jonas BM, Kubota K, Kuskowski MA, Boustany L, Shelton DL, Mantyh PW. *Anti-NGF therapy profoundly reduces bone cancer pain and the accompanying increase in markers of peripheral and central sensitization.* Pain. 2005 May;115(1-2):128-41.

Shelton DL, Zeller J, Ho WH, Pons J, Rosenthal A. *Nerve growth factor mediates hyperalgesia and cachexia in auto-immune arthritis.* Pain. 2005 Jul;116(1-2):8-16.

Shao C, Gao Y, Jin D, Xu X, Tan S, Yu H, Zhao Q, Zhao L, Wang W, Wang D. *DNMT3a methylation in neuropathic pain.* J Pain Res. 2017 Sep 18;10:2253-2262. doi: 10.2147/JPR.S130654. eCollection 2017.

Snipes GJ, Suter U. *Molecular anatomy and genetics of myelin proteins in the peripheral nervous system.* J Anat. 1995 Jun;186 (Pt 3):483-94.

Stanzel RD, Lourenssen S, Blennerhassett MG. *Inflammation causes expression of NGF in epithelial cells of the rat colon.* Exp Neurol. 2008 May;211(1):203-13. doi: 10.1016/j.expneurol.2008.01.028. Epub 2008 Feb 16.

Suter MR, Wen YR, Decosterd I, Ji RR. *Do glial cells control pain?* Neuron Glia Biol. 2007 Aug;3(3):255-68. doi: 10.1017/S1740925X08000100.

Svensson P, Cairns BE, Wang K, Arendt-Nielsen L. *Injection of nerve growth factor into human masseter muscle evokes long-lasting mechanical allodynia and hyperalgesia.* Pain. 2003 Jul;104(1-2):241-7.

Taves S, Berta T, Chen G, Ji RR. *Microglia and spinal cord synaptic plasticity in persistent pain.* Neural Plast. 2013;2013:753656. doi: 10.1155/2013/753656. Epub 2013 Aug 18.

Theoharides TC, Alysandratos KD, Angelidou A, Delivanis DA, Sismanopoulos N, Zhang B, Asadi S, Vasiadi M, Weng Z, Miniati A, Kalogeromitros D. *Mast cells and inflammation.* Biochim Biophys Acta.

2012 Jan;1822(1):21-33. doi: 10.1016/j.bbadis.2010.12.014. Epub 2010 Dec 23.

Treede RD, Jensen TS, Campbell JN, Cruccu G, Dostrovsky JO, Griffin JW, Hansson P, Hughes R, Nurmikko T, Serra J. *Neuropathic pain: redefinition and a grading system for clinical and research purposes.* Neurology. 2008 Apr 29;70(18):1630-5. Epub 2007 Nov 14.

Ugolini G, Marinelli S, Covaceuszach S, Cattaneo A, Pavone F. *The function neutralizing anti-TrkA antibody MNAC13 reduces inflammatory and neuropathic pain.* Proc Natl Acad Sci U S A. 2007 Feb 20;104(8):2985-90. Epub 2007 Feb 14.

Vacca V, Marinelli S, Pieroni L, Urbani A, Luvisetto S, Pavone F. *17beta-estradiol counteracts neuropathic pain: a behavioural, immunohistochemical, and proteomic investigation on sex-related differences in mice.* Sci Rep. 2016 Jan 8;6:18980. doi: 10.1038/srep18980

Waller A. *Experiments on the section of glossopharyngeal and hypoglossal nerves of the frog and observations uf the alternatives produced thereby in the structure of their primitive fibres.* Philos rans R Soc Lond B Biol Sci 1850; 140:423-429.

Wang J, Ma SH, Tao R, Xia LJ, Liu L, Jiang YH. *Gene expression profile changes in rat dorsal horn after sciatic nerve injury.* Neurol Res. 2017 Feb;39(2):176-182. doi: 10.1080/01616412.2016.1273590. Epub 2016 Dec 30.

Watanabe T, Ito T, Inoue G, Ohtori S, Kitajo K, Doya H, Takahashi K, Yamashita T. *The p75 receptor is associated with inflammatory thermal hypersensitivity.* J Neurosci Res. 2008 Dec;86(16):3566-74. doi: 10.1002/jnr.21808.

Watson CJ. *Insular balance of glutamatergic and GABAergic signaling modulates pain processing.* Pain. 2016 Oct;157(10):2194-207. doi: 10.1097/j.pain.0000000000000615.

Willis WD Jr. *Dorsal root potentials and dorsal root reflexes: a double-edged sword.* Exp Brain Res. 1999 Feb;124(4):395-421.

Wong KM, Babetto E, Beirowski B. *Axon degeneration: make the Schwann cell great again.* Neural Regen Res. 2017 Apr;12(4):518-524. doi: 10.4103/1673-5374.205000.

Woolf CJ, Safieh-Garabedian B, Ma QP, Crilly P, Winter J. *Nerve growth factor contributes to the generation of inflammatory sensory hypersensitivity.* Neuroscience. 1994 Sep;62(2):327-31.

Yousuf MS, Kerr BJ. *The Role of Regulatory Transporters in Neuropathic Pain*. Adv Pharmacol. 2016;75:245-71. doi: 10.1016/bs.apha.2015.12.003. Epub 2016 Jan 21.